affect the cross-bridge cycling and V_{max} but at different kinetic steps. Taken together our studies suggest that up-regulation of h1-CaP in the SM-B null mice may be a compensatory alteration to maintain a reduced level of cross-bridge cycling over time in the absence of SM-B myosin. However, reduction in the smooth muscle α-actin levels and increase in h-CaD levels suggest that changes in other contractile and regulatory proteins may also contribute to the altered contractile properties observed in the dKO bladder.

In addition to bladder, the contractile properties of mesenteric vessels were determined in the dKO mice. We have previously reported that SM-B myosin is expressed heterogeneously in the mesenteric vessels and contributes to their unique mechanical properties (Babu *et al.* 2004). In that study, we also found that loss of SM-B myosin resulted in increased force generation under isometric conditions (using wire-mounted vessel rings) in response to phenylephrine + potassium (Babu *et al.* 2004). In the present study, which used a more physiological pressurized vessel approach, maximal constriction to an activation cocktail containing high potassium (124 mM) and phenylephrine (10 μM) was similar in all treatment groups. Since the vessel is studied as an intact unit, the maximal extent of constriction, measured as the reduction in lumen diameter from a fully relaxed state, may be limited by other factors, e.g. cell–matrix interactions, rather than simply maximal force generation.

The (1) increased half-time to maximal constriction, and (2) reduced normalized slope of constriction observed in mesenteric vessels of both *smb*−/− and dKO mouse models, both suggest decreased shortening velocity of smooth muscle. These findings are consistent with our previous studies showing decreased shortening velocity in the mesenteric vessels with SM-B deficiency (Babu *et al.* 2001, 2004), and indicate that changes in h1-CaP do not seem to be the underlying cause for the altered kinetics in this type of smooth muscle. Another study using rat portal vein also showed that the maximal velocity of vascular smooth muscle shortening was independent of h1-CaP expression (Facemire *et al.* 2000).

The significantly reduced forced dilatation pressure in vessels from the *smb*−/− but not dKO mice was an unexpected finding that suggests that the modulatory effect of calponin on vascular smooth muscle (VSM) contractility may be influenced by (1) the extent of VSM activation, (2) spatial events such as the degree of actin–myosin overlap (the length–tension relationship), and (3) the nature of the distending force acting upon the vascular wall. All three possibilities derive from our use of the more physiological pressurized vessel methodology in this study, since earlier work used the isometric wire-mounted approaches in which vessels are stretched to a fixed length prior to activation and therefore unable to shorten in response to activation. In the pressurized vessel, as in the body, activation results in constriction, which is a reflection of smooth muscle shortening. This may have implications for the spatial relationship between actin, myosin and calponin, and thereby alter the nature of thin filament regulation, as there were no detectable differences in myosin heavy and light chain isoform expression. Further, in pressurized vessels, the force experienced by the vascular wall is true transmural pressure, which has a radial as well as a circumferential component that may influence the distribution of intramural stress. Although it was beyond the scope of this study to differentiate the ultrastructural/spatial *versus* biomechanical components of the response, these elements deserve consideration in future studies. Finally, although the velocity data were consistent with previous findings in mesenteric vessels (Babu *et al.* 2004) and in bladder smooth muscle (this study), it should be noted that, in arteries, the importance of shortening velocity *in vivo* is questionable, while the production and maintenance of force is essential to the maintenance of vascular tone and, thereby, peripheral resistance, blood pressure and normal organ perfusion. This differs from the bladder, whose proper function is dependent on smooth muscle shortening for effective micturition. Thus, it is not unreasonable to expect differences in the nature of h1-CaP regulation based on physiological function. Based on the results of our studies, h1-CaP appears to be a key regulator of both bladder and vascular smooth muscle contractility, although its precise modulatory role may clearly vary with smooth muscle tissue type and function.

References

Arner A, Lofgren M & Morano I (2003). Smooth, slow and smart muscle motors. *J Muscle Res Cell Motil* **24**, 165–173.

Babu GJ, Loukianov E, Loukianova T, Pyne GJ, Huke S, Osol G, Low RB, Paul RJ & Periasamy M (2001). Loss of SM-B myosin affects muscle shortening velocity and maximal force development. *Nat Cell Biol* **3**, 1025–1029.

Babu GJ, Pyne GJ, Zhou Y, Okwuchukuasanya C, Brayden JE, Osol G, Paul RJ, Low RB & Periasamy M (2004). Isoform switching from SM-B to SM-A myosin results in decreased contractility and altered expression of thin filament regulatory proteins. *Am J Physiol Cell Physiol* **287**, C723–C729.

Babu GJ, Warshaw DM & Periasamy M (2000). Smooth muscle myosin heavy chain isoforms and their role in muscle physiology. *Microsc Res Tech* **50**, 532–540.

D'Angelo G & Osol G (1993). Regional variation in resistance artery diameter responses to α-adrenergic stimulation during pregnancy. *Am J Physiol Heart Circ Physiol* **264**, H78–H85.

DiSanto ME, Cox RH, Wang Z & Chacko S (1997). NH2-terminal-inserted myosin II heavy chain is expressed in smooth muscle of small muscular arteries. *Am J Physiol Cell Physiol* **272**, C1532–C1542.

EL-Mezgueldi M & Marston SB (1996). The effects of smooth muscle calponin on the strong and weak myosin binding sites of F-actin. *J Biol Chem* **271**, 28161–28167.

Facemire C, Brozovich FV & Jin JP (2000). The maximal velocity of vascular smooth muscle shortening is independent of the expression of calponin. *J Muscle Res Cell Motil* **21**, 367–373.

Fujishige A, Takahashi K & Tsuchiya T (2002). Altered mechanical properties in smooth muscle of mice with a mutated calponin locus. *Zool Sci* **19**, 167–174.

Haase H & Morano I (1996). Alternative splicing of smooth muscle myosin heavy chains and its functional consequences. *J Cell Biochem* **60**, 521–528.

Haeberle JR (1994). Calponin decreases the rate of cross-bridge cycling and increases maximum force production by smooth muscle myosin in an in vitro motility assay. *J Biol Chem* **269**, 12424–12431.

Horiuchi KY & Chacko S (1991). The mechanism for the inhibition of actin-activated ATPase of smooth muscle heavy meromyosin by calponin. *Biochem Biophys Res Commun* **176**, 1487–1493.

Itoh T, Suzuki S, Suzuki A, Nakamura F, Naka M & Tanaka T (1994). Effects of exogenously applied calponin on Ca^{2+}-regulated force in skinned smooth muscle of the rabbit mesenteric artery. *Pflugers Arch* **427**, 301–308.

Jaworowski A, Anderson KI, Arner A, Engstrom M, Gimona M, Strasser P & Small JV (1995). Calponin reduces shortening velocity in skinned taenia coli smooth muscle fibres. *FEBS Lett* **365**, 167–171.

Karagiannis P, Babu GJ, Periasamy M & Brozovich FV (2003). The smooth muscle myosin seven amino acid heavy chain insert's kinetic role in the crossbridge cycle for mouse bladder. *J Physiol* **547**, 463–473.

Karagiannis P, Babu GJ, Periasamy M & Brozovich FV (2004). Myosin heavy chain isoform expression regulates shortening velocity in smooth muscle: studies using an SMB KO mouse line. *J Muscle Res Cell Motil* **25**, 149–158.

Karagiannis P & Brozovich FV (2003). The kinetic properties of smooth muscle: how a little extra weight makes myosin faster. *J Muscle Res Cell Motil* **24**, 157–163.

Kelley CA, Takahashi M, Yu JH & Adelstein RS (1993). An insert of seven amino acids confers functional differences between smooth muscle myosins from the intestines and vasculature. *J Biol Chem* **268**, 12848–12854.

Lauzon AM, Trybus KM & Warshaw DM (1998*a*). Molecular mechanics of two smooth muscle heavy meromyosin constructs that differ by an insert in the motor domain. *Acta Physiol Scand* **164**, 357–361.

Lauzon AM, Tyska MJ, Rovner AS, Freyzon Y, Warshaw DM & Trybus KM (1998*b*). A 7-amino-acid insert in the heavy chain nucleotide binding loop alters the kinetics of smooth muscle myosin in the laser trap. *J Muscle Res Cell Motil* **19**, 825–837.

Lofgren M, Fagher K, Wede OK & Arner A (2002). Decreased shortening velocity and altered myosin isoforms in guinea-pig hypertrophic intestinal smooth muscle. *J Physiol* **544**, 707–714.

Matthew JD, Khromov AS, McDuffie MJ, Somlyo AV, Somlyo AP, Taniguchi S & Takahashi K (2000). Contractile properties and proteins of smooth muscles of a calponin knockout mouse. *J Physiol* **529**, 811–824.

Matthew JD, Khromov AS, Trybus KM, Somlyo AP & Somlyo AV (1998). Myosin essential light chain isoforms modulate the velocity of shortening propelled by nonphosphorylated cross-bridges. *J Biol Chem* **273**, 31289–31296.

Morgan KG & Gangopadhyay SS (2001). Invited review: cross-bridge regulation by thin filament-associated proteins. *J Appl Physiol* **91**, 953–962.

Rovner AS, Freyzon Y & Trybus KM (1997). An insert in the motor domain determines the functional properties of expressed smooth muscle myosin isoforms. *J Muscle Res Cell Motil* **18**, 103–110.

Siegman MJ, Butler TM, Mooers SU, Trinkle-Mulcahy L, Narayan S, Adam L, Chacko S, Haase H & Morano I (1997). Hypertrophy of colonic smooth muscle: contractile proteins, shortening velocity, and regulation. *Am J Physiol Gastrointest Liver Physiol* **272**, G1571–G1580.

Somlyo AV, Khromov AS, Webb MR, Ferenczi MA, Trentham DR, He ZH, Sheng S, Shao Z & Somlyo AP (2004). Smooth muscle myosin: regulation and properties. *Philos Trans R Soc Lond B Biol Sci* **359**, 1921–1930.

Somlyo AV, Matthew JD, Wu X, Khromov AS & Somlyo AP (1998). Regulation of the cross-bridge cycle: the effects of MgADP, LC17 isoforms and telokin. *Acta Physiol Scand* **164**, 381–388.

Takahashi K & Yamamura H (2003). Studies and perspectives of calponin in smooth muscle regulation and cancer gene therapy. *Adv Biophys* **37**, 91–111.

Takahashi K, Yoshimoto R, Fuchibe K, Fujishige A, Mitsui-Saito M, Hori M, Ozaki H, Yamamura H, Awata N, Taniguchi S, Katsuki M, Tsuchiya T & Karaki H (2000). Regulation of shortening velocity by calponin in intact contracting smooth muscles. *Biochem Biophys Res Commun* **279**, 150–157.

Uyama Y, Imaizumi Y, Watanabe M & Walsh MP (1996). Inhibition by calponin of isometric force in demembranated vascular smooth muscle strips: the critical role of serine-175. *Biochem J* **319**, 551–558.

Winder SJ, Allen BG, Clement-Chomienne O & Walsh MP (1998). Regulation of smooth muscle actin–myosin interaction and force by calponin. *Acta Physiol Scand* **164**, 415–426.

Yoshikawa H, Taniguchi SI, Yamamura H, Mori S, Sugimoto M, Miyado K, Nakamura K, Nakao K, Katsuki M, Shibata N & Takahashi K (1998). Mice lacking smooth muscle calponin display increased bone formation that is associated with enhancement of bone morphogenetic protein responses. *Genes Cells* **3**, 685–695.

Ackowledgements

This work was supported by American Heart Association Grant 0365173B (to G.J.B.), National Heart, Lung, and Blood Institute Grant HL-38355-17 (to M.P.) and HL-44181 (to F.V.B.).

JOURNAL OF VIROLOGY, Feb. 2006, p. 1476–1486 Vol. 80, No. 3
0022-538X/06/$08.00+0 doi:10.1128/JVI.80.3.1476–1486.2006

Herpes Simplex Virus 1-Encoded Protein Kinase UL13 Phosphorylates Viral Us3 Protein Kinase and Regulates Nuclear Localization of Viral Envelopment Factors UL34 and UL31

Akihisa Kato,[1,2]† Mayuko Yamamoto,[2]† Takashi Ohno,[1,2] Michiko Tanaka,[4] Tetsutaro Sata,[4] Yukihiro Nishiyama,[2] and Yasushi Kawaguchi[1,2,3]*

Department of Infectious Disease Control, International Research Center for Infectious Diseases, The Institute of Medical Science, The University of Tokyo, Minato-ku, Tokyo 108-8639,[1] Department of Virology, Nagoya University Graduate School of Medicine, Showa-ku, Nagoya 466-8550,[2] PRESTO, Japan Science and Technology Agency, Kawaguchi, Saitama, 332-0012,[3] and Department of Pathology, National Institute of Infectious Disease, Shinjuku-ku, Tokyo 162-8640,[4] Japan

Received 19 September 2005/Accepted 4 November 2005

UL13 and Us3 are protein kinases encoded by herpes simplex virus 1. We report here that Us3 is a physiological substrate for UL13 in infected cells, based on the following observations. (i) The electrophoretic mobility, in denaturing gels, of Us3 isoforms from Vero cells infected with wild-type virus was slower than that of isoforms from cells infected with a UL13 deletion mutant virus (ΔUL13). After treatment with phosphatase, the electrophoretic mobility of the Us3 isoforms from cells infected with wild-type virus changed, with one isoform migrating as fast as one of the Us3 isoforms from ΔUL13-infected cells. (ii) A recombinant protein containing a domain of Us3 was phosphorylated by UL13 in vitro. (iii) The phenotype of ΔUL13 resembles that of a recombinant virus lacking the Us3 gene (ΔUs3) with respect to localization of the viral envelopment factors UL34 and UL31, whose localization has been shown to be regulated by Us3. UL34 and UL31 are localized in a smooth pattern throughout the nuclei of cells infected with wild-type virus, whereas their localization in ΔUL13- and ΔUs3-infected cells appeared as nuclear punctate patterns. These results indicate that UL13 phosphorylates Us3 in infected cells and regulates UL34 and UL31 localization, either by phosphorylating Us3 or by a Us3-independent mechanism.

Herpes simplex virus 1 (HSV-1) encodes at least three protein kinases, UL13, Us3, and UL39 (63). This report presents studies of the interaction between UL13 and Us3. The background for these studies is as follows.

First, UL13 is a serine/threonine protein kinase that is packaged in the tegument, a virion structural component located between the nucleocapsid and the envelope (9, 12, 13, 29, 52, 68). UL13 plays a role in viral replication in cell cultures, since UL13 deletion mutants exhibit impaired replication in some cell lines, including rabbit skin cells and baby hamster kidney (BHK) cells (10, 45, 56, 57, 70). Although the mechanism by which UL13 acts in HSV-1-infected cells remains unclear, infection of rabbit skin cells and BHK cells with UL13 deletion mutants reduces the expression levels of the α protein ICP0 and a subset of γ proteins, including UL26, UL26.5, UL38, UL41, and Us11 (56), suggesting that UL13 is involved in viral-gene expression in infected cells. UL13 would also be expected to function in early postinfection events, since tegument proteins are, in general, released into the cytoplasm of newly infected cells. In agreement with this possibility, phosphorylation of a tegument protein by UL13 has been implicated in promoting tegument disassembly in vitro (40).

* Corresponding author. Mailing address: Department of Infectious Disease Control, International Research Center for Infectious Diseases, The Institute of Medical Science, The University of Tokyo, 4-6-1 Shirokanedai, Minato-ku, Tokyo 108-8639, Japan. Phone: 81-3-6409-2070. Fax: 81-3-6409-2072. E-mail: ykawagu@ims.u-tokyo.ac.jp.

† A.K. and M.Y. contributed equally to this work.

Second, UL13 may function by phosphorylating specific viral and cellular proteins. Thus far, gI/gE, ICP0, ICP22, Us1.5, UL47, UL49, p60, elongation factor 1δ (EF-1δ), casein kinase IIβ subunit, and RNA polymerase II have been reported to be putative substrates for UL13 (4, 10, 20, 29, 32, 37, 44, 51, 57, 63). However, the biological significance of UL13-mediated phosphorylation in infected cells remains unclear. Since the UL13 amino acid sequence is conserved in all *Herpesviridae* subfamilies (9, 68), UL13 homologues may play a conserved role in herpesvirus replication by phosphorylating common host cellular targets and conserved herpesvirus gene products. The only substrate identified to date that is targeted by UL13 homologues from all *Herpesviridae* subfamilies is the cellular translation factor EF-1δ (26, 29, 30, 32). An interesting feature of the interaction between UL13 homologues and EF-1δ is that both cellular protein kinase cdc2 and UL13 homologues phosphorylate the same EF-1δ amino acid residue (29). These observations suggest that UL13 homologues may share a function that mimics the cellular cdc2 protein kinase (28). This hypothesis is supported by data showing that HSV-1 UL13 phosphorylates the cdc2 site of the casein kinase IIβ subunit in vitro (29). Moreover, reports that the Epstein-Barr virus (EBV) UL13 homologue BGLF4 and cdc2 phosphorylate the same sites of EBV regulatory proteins— EBNA-LP and EBNA-2, which are critical for the transcriptional activities of the proteins—both in vitro and in vivo are consistent with this hypothesis (27, 75, 76).

Third, Us3 is also a serine/threonine protein kinase and is packaged in the virion (18, 55, 62). In contrast to UL13, the

Us3 amino acid sequence is conserved only in the subfamily *Alphaherpesvirinae* (9, 39, 63, 68), and the function of Us3 as a virion component has not been elucidated yet. Us3 is a positive regulator of viral replication, based on studies showing that recombinant Us3 mutant viruses have impaired growth properties in cell cultures and mouse models (49, 62, 65). Increasing data indicate that Us3 plays a role in viral replication by regulating apoptosis. It has been reported that Us3 protein kinase can prevent apoptosis induced by proapoptotic cellular proteins, osmotic shock, and replication-incompetent mutant virus (2, 6, 7, 23, 36, 41–43, 50). Benetti and Roizman have recently shown that Us3 activates protein kinase A (PKA), a cellular cyclic-AMP-dependent protein kinase with phosphorylation target sequences resembling those of Us3, and that both Us3 and PKA phosphorylate the same target protein residues (3). Us3 may express its antiapoptotic activity through phosphorylation of PKA substrates, by activating PKA, and/or by mimicking this cellular protein kinase.

Fourth, Us3 is involved in the nuclear egress of progeny nucleocapsids based on several observations. (i) In cells infected with mutant virus lacking functional Us3, virions were found to accumulate in the perinuclear space in large invaginations of the inner nuclear membrane (62). Similar structures were reported in cells infected with a recombinant pseudorabies virus, a member of *Alphaherpesvirinae*, lacking a Us3-homologous gene (34, 71). (ii) Us3 phosphorylates UL34 and UL31 (25, 58, 65), both of which are critical regulators for primary envelopment of nucleocapsids at the nuclear membrane (61, 64, 74). (iii) Us3 protein kinase activity is required for proper localization of UL34 and UL31 at the nuclear membrane (61, 62, 65). Us3 may function in the nuclear egress pathway by direct or indirect interactions with UL34 and UL31.

We report here studies showing that UL13 phosphorylates Us3 in infected cells and examine some possible effects of this phorphorylation.

MATERIALS AND METHODS

Cells and viruses. Vero and *Spodoptera frugiperda* Sf9 cells were described previously (29, 69). A human neuroblastoma cell line (SK-N-SH cells) was kindly provided by B. Roizman (University of Chicago, Chicago, Ill.) and maintained in Dulbecco's modified Eagle medium (DMEM) containing 10% fetal calf serum (FCS). The HSV-1 wild-type strain HSV-1(F) and UL13 deletion mutant virus R7356 were described previously (17, 29, 56, 69). The Us3 deletion mutant virus R7041 (55) was kindly provided by B. Roizman. The recombinant baculoviruses Bac-GST-UL13 and Bac-GST-UL13K176M were described previously (29).

Plasmids. pBluescript II KS(+) (Stratagene) was digested with HindIII, treated with T4 DNA polymerase, and religated to produce pBluescript II KS(+) without the HindIII site. The resultant plasmid was designated pBSΔHdIII. BglII O in pBSΔHdIII was generated by cloning the 5.4-kbp BglII O fragment of pBC1015 (32) into the BamHI site of pBSΔHdIII. pMAL-Us3-P1 and pMAL-Us3-P2 were constructed by amplifying the domains encoding Us3 codons 405 to 481 and codons 254 to 411, respectively, by PCR from pBC1013 (33) and cloning the DNA fragments into pMAL-c (New England BioLabs) in frame with maltose binding protein (MBP). pBC1013 and pBC1015 were kindly provided by B. Roizman.

Generation of a recombinant virus. To construct the recombinant virus R7356Rep with a repaired UL13 gene, the UL13 sequences deleted from R7356 were restored by cotransfecting rabbit skin cells with R7356 DNA and BglII O in pBSΔHdIII. Plaques were isolated, purified, and screened by PCR analysis for wild-type UL13 sequences. Restoration of the original sequence was confirmed by Southern blotting.

Purification of GST fusion proteins from baculovirus-infected cells. The glutathione *S*-transferase (GST)-UL13 and GST-UL13K176M proteins were purified from Sf9 cells infected with Bac-GST-UL13 and Bac-GST-UL13K176M, respectively, as described previously (29).

Production and purification of MBP fusion proteins. MBP fusion proteins (MBP-Us3-P1, MBP-Us3-P2, and MBP-LacZ) were expressed in *Escherichia coli* that had been transformed with pMAL-Us3-P1, pMAL-Us3-P2, and pMAL-c, respectively, and purified as described previously (29).

Antibodies. Rabbit polyclonal antibodies to Us3, UL34, and UL31 were described previously (14, 21, 25, 66, 78). Chicken polyclonal antibody to UL34 (61) was kindly provided by R. Roller (University of Iowa). Mouse monoclonal antibody to nucleoporin p62 was purchased from Transduction Laboratories.

In vitro kinase assays. MBP fusion proteins were captured on amylose beads (New England BioLabs) and used as substrates in in vitro kinase assays with 2 μg of purified GST-UL13 and GST-UL13K176M, as described previously (29). The relative amounts of radioactivity in substrates phosphorylated by GST-UL13 were quantified with the aid of Dolphin Doc and the software Dolphin-1D (Wealtec).

Immune complex kinase assays. Vero cells were infected with either HSV-1(F), R7041, or R7356 at a multiplicity of infection (MOI) of 5 PFU per cell. Infected cells were harvested at 12 h postinfection and lysed in radioimmunoprecipitation assay (RIPA) buffer (50 mM Tris-HCl [pH 7.5], 150 mM NaCl, 1% Nonidet P-40 [NP-40], 0.5% deoxycholate, 0.1% sodium dodecyl sulfate) containing a protease inhibitor cocktail (Sigma). Supernatant fluids obtained after centrifugation of the cell lysate were precleared by incubation with protein A-Sepharose beads (Amersham-Pharmacia) at 4°C for 30 min and then reacted with rabbit polyclonal antibody to Us3 at 4°C for 2 h. Additional protein A-Sepharose beads were added, and the reaction continued for another 1.5 h. Immunoprecipitates were collected by a brief centrifugation; washed twice with high-salt buffer (1 M NaCl, 10 mM Tris-HCl [pH 8.0], 0.2% NP-40), once with low-salt buffer (0.1 M NaCl, 10 mM Tris-HCl [pH 8.0], 0.2% NP-40), six times with RIPA buffer, and twice with Us3 kinase buffer (50 mM Tris-HCl [pH 9.0], 20 mM $MgCl_2$, 0.1% NP-40, and 1 mM dithiothreitol) (25); and analyzed by in vitro kinase assays. For these assays, Us3 kinase buffer containing 10 μM ATP and 10 μCi [γ-^{32}P]ATP was added to the protein A-Sepharose beads (15 μl) containing immunoprecipitated Us3 protein kinase, and the samples were reacted at 30°C for 30 min. After incubation, the samples were washed twice with TNE buffer (20 mM Tris-HCl [pH 8.0], 100 mM NaCl, and 1 mM EDTA) and analyzed by electrophoresis in denaturing gels with or without phosphatase treatment. After electrophoresis, the separated proteins were transferred from the gels to nitrocellulose membranes (Bio-Rad), and the membranes were exposed to X-ray film and then immunoblotted with anti-Us3 antibody.

Phosphatase treatment. After the in vitro kinase assays, the MBP fusion proteins or immunoprecipitates were washed twice with TNE buffer and twice with lambda protein phosphatase (λ-PPase) reaction buffer supplemented with 2 mM $MnCl_2$ (New England BioLabs). Then, λ-PPase reaction buffer containing 2,000 U λ-PPase (New England BioLabs) was added to the beads, and the samples were incubated at 37°C for 30 min. For MBP fusion proteins, after electrophoresis in denaturing gels, the gel was stained with Coomassie brilliant blue (CBB) and exposed to X-ray film. For immunoprecipitates, the samples were electrophoretically separated and transferred to nitrocellulose membranes, and the membranes were exposed to X-ray film and then immunoblotted with anti-Us3 antibody. In other studies, infected cells were lysed in NP-40 buffer (10 mM Tris-HCl [pH 7.8], 0.15 M NaCl, 1 mM EDTA, and 1% NP-40) containing a protease inhibitor cocktail. The supernatants obtained after centrifugation of the cell lysates were incubated with 20 U alkaline phosphatase (CIP; New England BioLabs) for 2 h at 37°C, after which they were electrophoretically separated and then immunoblotted with anti-Us3 antibody.

Southern blotting, immunoblotting, and immunofluorescence. Southern blotting and immunoblotting were performed as described previously (24, 69). Indirect immunofluorescence assays were performed as described previously (31), except that anti-mouse or anti-rabbit immunoglobulin G (IgG) conjugated to Alexa Fluor 488, anti-rabbit IgG conjugated to Alexa Fluor 546, or anti-chicken IgG conjugated to fluorescein isothiocyanate (FITC) was used as a secondary antibody, in addition to anti-rabbit IgG conjugated to FITC, and samples were examined with a Zeiss LSM510 or LSM5 laser scanning microscope.

Induction of apoptosis and measurement of caspase 3/7 activity. SK-N-SH cells were mock infected or infected with HSV-1(F), R7041, or R7356 at an MOI of 5. After a 1-h virus adsorption, the virus inoculum was replaced with DMEM containing 10% FCS. At 12 h postinfection, the cell culture medium was removed and the cells were exposed to 1 M sorbitol in DMEM containing 1% FCS for 1 h to produce osmotic shock and induce apoptosis. After sorbitol treatment, the cells were washed with DMEM and incubated in DMEM containing 1% FCS for an additional 5 h. The cells were then harvested and assayed for caspase 3/7 activity using a Caspase-Glo 3/7 assay kit with a tetrapeptide (Z-DEVD)-conju-

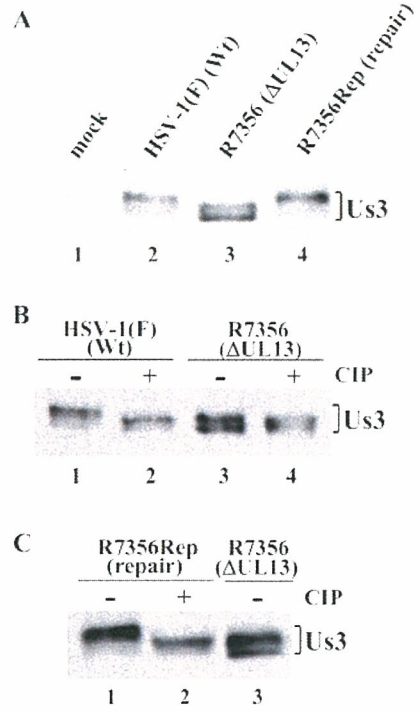

FIG. 1. (A) Immunoblot of electrophoretically separated lysates from Vero cells mock infected (lane 1) or infected with HSV-1(F) (lane 2), R7356 (lane 3), or R7356Rep (lane 4). Infected cells were harvested at 12 h postinfection and analyzed by immunoblotting with polyclonal antibody to Us3. Wt, wild type. (B) Immunoblots of electrophoretically separated lysates from Vero cells infected with HSV-1(F) (lanes 1 and 2) and R7356 (lanes 3 and 4). The infected cells were harvested at 12 h postinfection, solubilized, mock treated (lanes 1 and 3) or treated with CIP (lanes 2 and 4), and immunoblotted with antibody to Us3. (C) Immunoblots of electrophoretically separated lysates from Vero cells infected with R7356Rep (lanes 1 and 2) and R7356 (lane 3). The infected cells were harvested at 12 h postinfection, solubilized, mock treated (lanes 1 and 3) or treated with CIP (lane 2), and immunoblotted with antibody to Us3.

gated aminoluciferin substrate, according to the manufacturer's instructions (Promega).

RESULTS

UL13 mediates phosphorylation of Us3 in infected cells. For these experiments, Vero cells were mock infected or infected with wild-type virus [HSV-1(F)], UL13 deletion mutant virus (R7356), or UL13-repaired R7356 virus (R7356Rep) at an MOI of 5; harvested at 12 h postinfection; solubilized; and analyzed by immunoblotting with polyclonal antibody to Us3. As reported previously (41), Us3 protein from HSV-1(F)-infected Vero cells was detected in a denaturing gel as doublet bands, with the more slowly migrating isoform predominating (Fig. 1A, lane 2). In R7356-infected Vero cells, the Us3 protein was also detected as doublet bands, but the amounts of Us3 in the two isoforms were more equal than in HSV-1(F)-infected cells, and both isoforms from R7356-infected cells appeared to migrate faster than those from HSV-1(F)-infected cells (Fig. 1A, lanes 2 and 3).

To verify that the phenotype observed in these studies was due to the UL13 deletion, this deletion in the R7356 mutant virus was repaired to yield the UL13 repaired virus R7356Rep, as described in Materials and Methods. The genotype of R7356Rep was confirmed by Southern blotting when restricted with BglII and probed with the BglII O DNA fragment (data not shown). The electrophoretic pattern of Us3 isoforms from R7356Rep-infected cells could not be differentiated from that of Us3 isoforms from cells infected with wild-type virus (Fig. 1A, lanes 2 and 4). These results indicate that UL13 mediates posttranslational processing of Us3 in HSV-infected cells.

To examine whether the UL13-mediated posttranslational processing of Us3 is due to phosphorylation, the infected-cell lysates were phosphatase treated with CIP, solubilized, and analyzed by immunoblotting with polyclonal antibody to Us3. After CIP treatment, the electrophoretic mobilities of both Us3 isoforms from Vero cells infected with wild-type HSV-1(F) or UL13 repaired R7356Rep virus changed, with one of the Us3 isoforms migrating as fast as one from R7356-infected cells (Fig. 1B, lanes 1 to 3, and Fig. 1C, lanes 1 to 3). CIP treatment of lysate from cells infected with R7356 had little effect on the migration of the Us3 isoforms (Fig. 1B, lanes 3 and 4). These results indicate that UL13 mediates phosphorylation of Us3 in infected cells. Consistent with our observations, Poon and Roizman (54) recently reported that Us3 proteins produced by cells infected with the UL13 deletion mutant virus R7356 migrated in a denaturing gel faster than those produced by cells infected with wild-type virus. However, the study did not address whether the wild-type phenotype was restored in cells infected with a recombinant virus in which the UL13 sequence was repaired and whether the posttranslational modification of Us3 mediated by UL13 was due to phosphorylation (54).

UL13 phosphorylates Us3 in vitro. To investigate whether UL13 directly phosphorylates Us3, we generated and purified chimeric proteins consisting of MBP fused to peptides encoded by Us3 codons 254 to 411 (MBP-Us3-P2) and codons 405 to 481 (MBP-Us3-P1) (Fig. 2A). We also used MBP-LacZ protein (25) as a control. MBP-Us3-P1, MBP-Us3-P2, and MBP-LacZ contain 45, 56, and 47 serines/threonines, respectively. The MBP fusion proteins were captured on amylose beads and used as substrates in in vitro kinase assays with purified wild-type GST-UL13 or the kinase-negative mutant GST-UL13K176M. As shown in Fig. 2C, MBP-Us3-P1 was labeled with [γ-^{32}P]ATP in kinase assays using GST-UL13 (Fig. 2C, lane 3), while the MBP-Us3-P2 and MBP-LacZ proteins were not (Fig. 2C, lanes 1 and 5). When the gel was overexposed, the MBP-LacZ was labeled very faintly in the presence of GST-UL13 (data not shown). However, the relative amount of radioactivity in MBP-Us3-P1 was >100 higher than that in MBP-LacZ (data not shown). When the kinase-negative mutant GST-UL13K176M was used, none of the MBP fusion proteins were labeled (Fig. 2C, lanes 2, 4, and 6). To confirm that MBP-Us3-P1 labeling by GST-UL13 was due to phosphorylation, the labeled MBP-Us3-P1 was treated with λ-PPase. As shown in Fig. 2E, MBP-Us3-P1 labeling by GST-UL13 was eliminated by phosphatase treatment, indicating that MBP-Us3-P1 was labeled by phosphorylation. The presence of each MBP fusion protein and the radiolabeled MBP-Us3-P1 band was verified by CBB staining (Fig. 2B and D).

These results indicate that UL13 specifically and directly

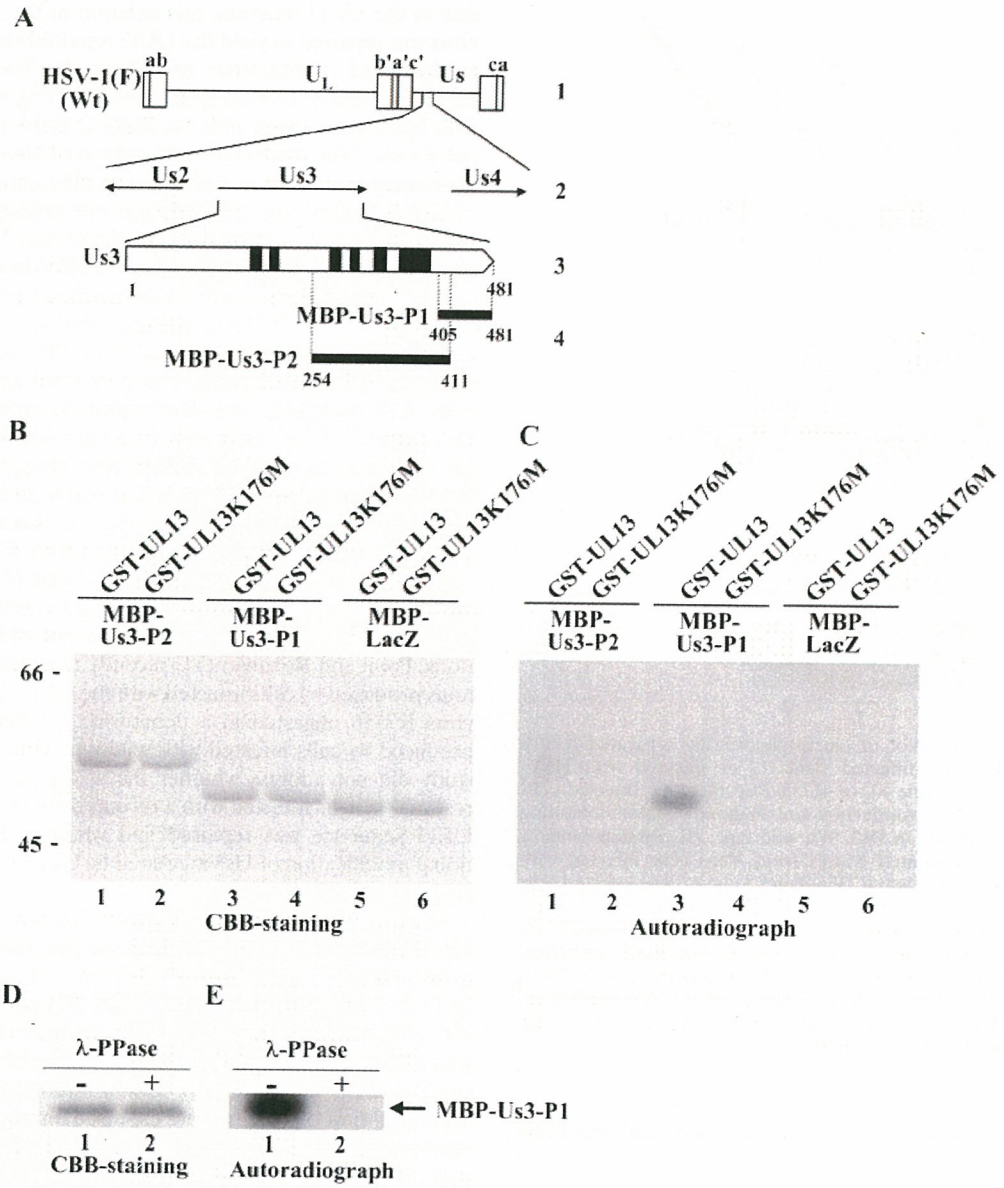

FIG. 2. (A) Schematic diagram of the genome structures of wild-type (Wt) virus HSV-1(F) and the location of the Us3 gene. Line 1, linear representation of the HSV-1(F) genome. The unique sequences are represented as unique long (U_L) and short (Us) domains, and the terminal repeats flanking them are shown as open rectangles with the designation above each repeat. Line 2, structure of the genome domain containing the Us2, Us3, and Us4 open reading frames. Line 3, structure of the Us3 open reading frame. The shaded areas represent subdomains I to VI, which are conserved in eukaryotic protein kinases (68). Line 4, the domains of the Us3 gene used in these studies to generate MBP-Us3 fusion proteins. (B) CBB-stained images of phosphorylated Us3. Purified MBP-Us3-P2 (lanes 1 and 2), MBP-Us3-P1 (lanes 3 and 4), and MBP-LacZ (lanes 5 and 6) incubated in kinase buffer containing [γ-^{32}P]ATP and purified GST-UL13 (lanes 1, 3, and 5) or GST-UL13K176M (lanes 2, 4, and 6), separated on a denaturing gel, and stained with CBB. Molecular masses (kDa) are shown on the left. (C) Autoradiograph of the gel in panel B. (D) Purified MBP-Us3-P1 incubated in kinase buffer containing [γ-^{32}P]ATP and purified GST-UL13 and then either mock treated (lane 1) or treated with λ-PPase (lane 2), separated on a denaturing gel, and stained with CBB. (E) Autoradiograph of the gel in panel D.

phosphorylates the Us3 peptide encoded by codons 405 to 481 in vitro.

UL13-mediated phosphorylation of Us3 does not affect Us3 protein kinase activity in infected cells. Phosphorylation of a protein often leads to a change in function(s) of the target protein. The result, described above, showing that Us3 is phosphorylated by UL13 suggested three possible effects of this modification: (i) UL13 may affect the intrinsic protein kinase activity of Us3, (ii) UL13 may affect the ability of Us3 to regulate apoptosis, and (iii) UL13 may affect the ability of Us3 to determine the localization of UL31 and UL34.

To test the first possibility, two series of experiments were done. In the first, Vero cells infected with HSV-1(F), R7041 (ΔUs3), or R7356 (ΔUL13) were harvested at 12 h postinfec-

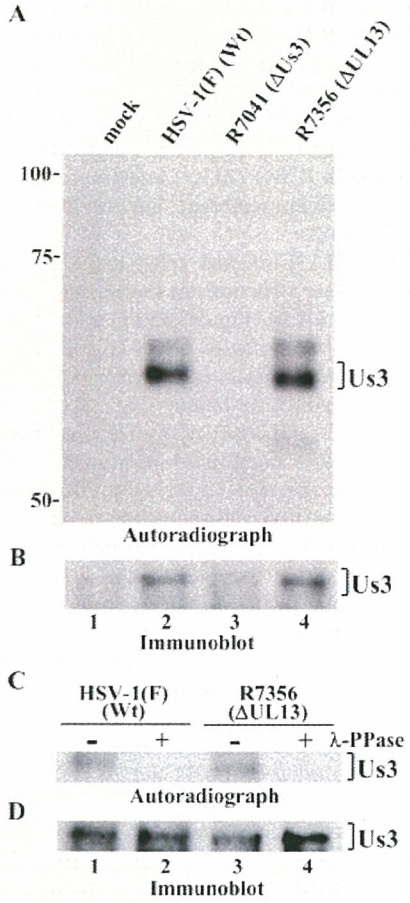

FIG. 3. Autoradiographic images of Us3 immunoprecipitates subjected to in vitro kinase assay. (A) Vero cells were mock infected (lane 1) or infected with HSV-1(F) (lane 2), R7041 (lane 3), or R7356 (lane 4); harvested at 12 h postinfection; and immunoprecipitated with antibody to Us3. The immunoprecipitates were incubated in kinase buffer containing [γ-^{32}P]ATP, separated on a denaturing gel, transferred to a nitrocellulose membrane, and analyzed by autoradiography. (B) Immunoblot of the nitrocellulose membrane in panel A using anti-Us3 antibody. (C) Immunoprecipitates prepared as in panel A were either mock treated (lanes 1 and 3) or treated with λ-PPase (lanes 2 and 4), separated on a denaturing gel, transferred to a nitrocellulose membrane, and analzyed by autoradiography. Wt, wild type. (D) Immunoblot of the nitrocellulose membrane in panel C using anti-Us3 antibody.

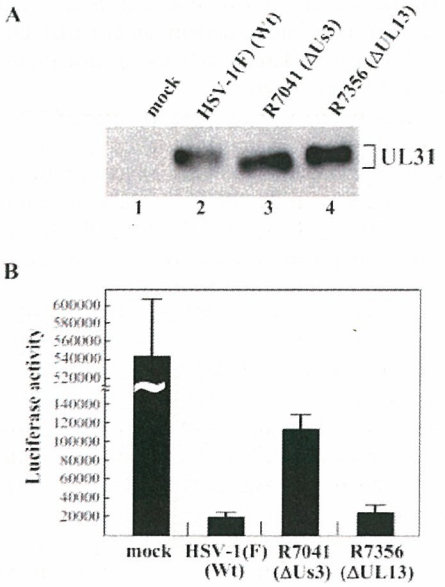

FIG. 4. (A) Immunoblot of electrophoretically separated lysates from Vero cells mock infected (lane 1) or infected with HSV-1(F) (lane 2), R7041 (lane 3), or R7356 (lane 4) at an MOI of 5. Infected cells were harvested at 12 h postinfection and immunoblotted with anti-UL31 antibody. (B) Caspase 3/7 activity of infected SK-N-SH cells after induction of apoptosis by osmotic shock. SK-N-SH cells were mock infected or infected with HSV-1(F), R7041, or R7356. At 12 h postinfection, the cells were exposed to sorbitol for 1 h, incubated for an additional 5 h, harvested, and assayed for caspase 3/7 activity using a Z-DEVD-aminoluciferin substrate. The values are the means and standard deviations for three independent experiments. Wt, wild type.

tion, solubilized, and immunoprecipitated with antibody to Us3. The immunoprecipitates were then used in kinase assays. To reduce the possibility that the anti-Us3 antibody might bring down contaminating kinase(s), the immunoprecipitates containing Us3 protein kinase were washed with high-salt buffer containing 1 M NaCl prior to in vitro kinase assays. As shown in Fig. 3A, Us3 protein in immunoprecipitates from HSV-1(F)- and R7356 (ΔUL13)-infected cells were labeled with [γ-^{32}P]ATP at similar levels, but no labeled protein bands at the apparent M_r corresponding to Us3 were detected in immunoprecipitates from R7041 (ΔUs3)-infected cells. The labeling of Us3 proteins was due to phosphorylation, as determined by studies showing that the labeling was eliminated by phosphatase treatment (Fig. 3C). The expression of each Us3 protein and identification of the Us3 radiolabeled band were verified by immunoblotting (Fig. 3B and D). These results indicate that Us3 proteins in lysates from cells infected with HSV-1(F) and R7356 (ΔUL13) have similar autophosphorylation activities.

We recently reported that Us3 directly phosphorylates UL31 in vitro and mediates posttranslational processing of UL31, which involves phosphorylation, in infected cells (25). To examine whether UL13 affects the posttranslational modification of UL31 in infected cells, in a second series of experiments, Vero cells mock infected or infected with HSV-1(F), R7041 (ΔUs3), or R7356 (ΔUL13) were harvested at 12 h postinfection, solubilized, electrophoretically separated in a denaturing gel, and subjected to immunoblotting with antibody to UL31. These data showed that UL31 protein produced in cells infected with R7041 (ΔUs3) migrated faster than that produced in cells infected with HSV-1(F) (Fig. 4A, lanes 2 and 3). In contrast, UL31 from cells infected with R7356 (ΔUL13) migrated as slowly as UL31 from cells infected with HSV-(F) (Fig. 4A, lanes 2 and 4). These results suggest that Us3 proteins expressed in cells infected with wild-type virus and UL13 deletion mutant virus induce similar posttranslational modifications of UL31.

Taken together, these experiments suggest that UL13-mediated phosphorylation of Us3 is not required for optimal Us3 protein kinase activity in infected cells. However, we cannot completely exclude the possibility that UL13 affects the Us3

protein kinase activity in vivo if cofactors are necessary for optimal Us3 protein kinase activity and/or that UL13 modulates the Us3 protein kinase activity against other Us3 substrates, except UL31, in vivo.

Level of caspase 3/7 activity in virus-infected SK-N-SH cells in which apoptosis was induced. To investigate whether UL13-mediated phosphorylation of Us3 affects Us3 regulation of apoptosis in infected cells, SK-N-SH cells were infected with HSV-1(F), R7041 (ΔUs3), or R7356 (ΔUL13), and at 12 h postinfection, apoptosis was induced by osmotic shock. The cells were then harvested and assayed for caspase 3/7 activity. As shown in Fig. 4B, caspase 3/7 activity induced by osmotic shock was significantly reduced (26.3-fold) in HSV-1(F)-infected cells (Fig. 4B). In R7041 (ΔUs3)-infected cells, there was less reduction of caspase 3/7 activity (4.7-fold), probably due to the lack of Us3 antiapoptotic activity. Similar results were reported previously (7). In R7356 (ΔUL13)-infected cells, caspase 3/7 activity was similar to that in HSV-1(F)-infected cells. The activity of Us3 to regulate apoptosis was not detected in SK-N-SH cells without induction of apoptosis, based on the observation that the level of the caspase 3/7 activity in SK-N-SH cells infected with R7041 (ΔUs3), without osmotic shock, was comparable to that in cells infected with wild-type virus (data not shown). These results suggest that the presence of UL13 does not affect caspase 3/7 activity in infected SK-N-SH cells.

UL13 is required for proper localization of UL34 and UL31 in infected cells. To investigate whether UL13-mediated phosphorylation of Us3 affects the role of Us3 in UL34 and UL31 localization, Vero cells were mock infected or infected with HSV-1(F), R7041 (ΔUs3), R7356 (ΔUL13), or R7356Rep (repair) at an MOI of 5; fixed at 12 or 15 h postinfection; and processed for indirect immunofluorescence assay with antibodies to UL34, UL31, and nucleoporin p62.

Previous studies reported that in HSV-1(F)-infected Vero and HEp-2 cells at 8 and 12 h postinfection, the UL34 and UL31 proteins colocalize at the nuclear envelope in a uniform distribution (61, 65). However, as shown in Fig. 5, the UL34 and UL31 distributions observed in the studies reported here differed from those results (61, 65), with both UL34 and UL31 showing nucleoplasmic localization in addition to nuclear-membrane localization (Fig. 5A, E, I, and M). The antibodies to UL34 and UL31 used in these studies were not able to detect any specific fluorescence in mock-infected cells (data not shown). In R7041 (ΔUs3)-infected cells, in agreement with previous reports (61, 65), UL34 and UL31 proteins were detected as punctate structures at the nuclear membrane (Fig. 5B, F, J, and N). However, although the previous studies found only UL34 and UL31 localized at the nuclear membrane in R7041 (ΔUs3)-infected cells, in the studies reported here, UL34 and UL31 were also detected as punctate structures in the nucleoplasm of R7041 (ΔUs3)-infected cells (Fig. 5B, F, J, and N). The nucleoplasmic staining of UL34 and UL31 in HSV-1(F)- and R7041 (ΔUs3)-infected cells did not appear to be specific to rabbit polyclonal antibodies generated in our laboratory. Thus, in HSV-1(F)- or R7041 (ΔUs3)-infected cells, the patterns of UL34 fluorescence detected by chicken polyclonal antibody to UL34, which was used in previously published studies (61, 62, 65), were almost identical to those of UL34 fluorescence detected by rabbit polyclonal antibody to UL34 generated in our laboratory (Fig. 6A, a, b, d, and e). As reported earlier (61), UL34 detected by chicken polyclonal antibody was clearly colocalized with UL31 detected by rabbit polyclonal antibody to UL31 in discrete punctate structures of R7041 (ΔUs3)-infected cells (Fig. 6B, b, f, and j). However, in the studies reported here, the punctate regions containing both UL34 and UL31 in R7041 (ΔUs3)-infected cells were detected not only at the nuclear membrane, but also in the nucleoplasm (Fig. 6B, b, f, and j).

In R7356 (ΔUL13)-infected cells, the UL34 protein was detected as punctate structures in the nucleus by rabbit polyclonal antibody to UL34 (Fig. 5C and G and 6A, c), as well as chicken polyclonal antibody to UL34 (Fig. 6A, f, and 6B, c). Similarly, R7356 (ΔUL13)-infected cells showed UL31 localization as nuclear punctate staining (Fig. 5K and O and 6B, g). Furthermore, UL34 and UL31 colocalized in the nuclear punctate structures of R7356 (ΔUL13)-infected cells (Fig. 6B, c, g, and k). These localization features of UL34 and UL31 in R7356 (ΔUL13)-infected cells seemed to be similar to those of the viral proteins in R7041 (ΔUs3)-infected cells (61). It should be noted, however, that the sizes of UL34 and UL31 stained speckles in R7356 (ΔUL13)-infected cells appeared to be larger than those in R7041 (ΔUs3)-infected cells, and the number of speckles in R7356 (ΔUL13)-infected cells was less than in R7041 (ΔUs3)-infected cells (Fig. 5B, C, F, G, J, K, N, and O and 6A, b, c, e, and f, and B, b, c, f, g, j, and k). Furthermore, it appeared that the effect of UL13 deletion on localization of UL31 was less than that on UL34 at 12 h postinfection. Thus, in most (approximately 80%) of the R7356 (ΔUL13)-infected cells, the UL34 protein appeared as punctate structures in the nucleus, but in the remainder (approximately 20%), UL34 staining was similar to that in HSV-1(F)-infected cells (Fig. 5C and G). In contrast, most (approximately 80%) R7356 (ΔUL13)-infected cells showed UL31 localization similar to that in HSV-1(F)-infected cells, and the remainder (approximately 20%) showed UL31 localization as nuclear punctate staining (Fig. 5K and O). At later times of infection (15 h postinfection), however, the UL31 protein appeared as punctate structures in the nuclei of most R7356 (ΔUL13)-infected cells, as observed with the UL34 protein (Fig. 6B, c to g).

As expected, in R7356Rep-infected cells with the UL13 deletion repaired, UL34 and UL31 localization was similar to that in HSV-1(F)-infected cells, confirming that the change in localization of UL34 and UL31 proteins in R7356 (ΔUL13)-infected cells was a result of the deletion of the UL13 open reading frame (Fig. 5D, H, L, and P and 6B, d, h, and l). Nucleoporin p62, a marker for the nuclear envelope, was evenly distributed in HSV-1(F)-, R7041 (ΔUs3)-, R7356 (ΔUL13)-, and R7356Rep-infected cells (Fig. 5Q, R, S, and T). These results indicate that UL13 plays a role in the proper localization of UL34 and UL31 in HSV-1-infected cells.

DISCUSSION

Cellular protein kinases are often regulated by phosphorylation cascades organized by other protein kinases (15, 77). The question we have investigated in the studies reported here is whether one HSV-encoded protein kinase can target another HSV-encoded protein kinase and what effect this might

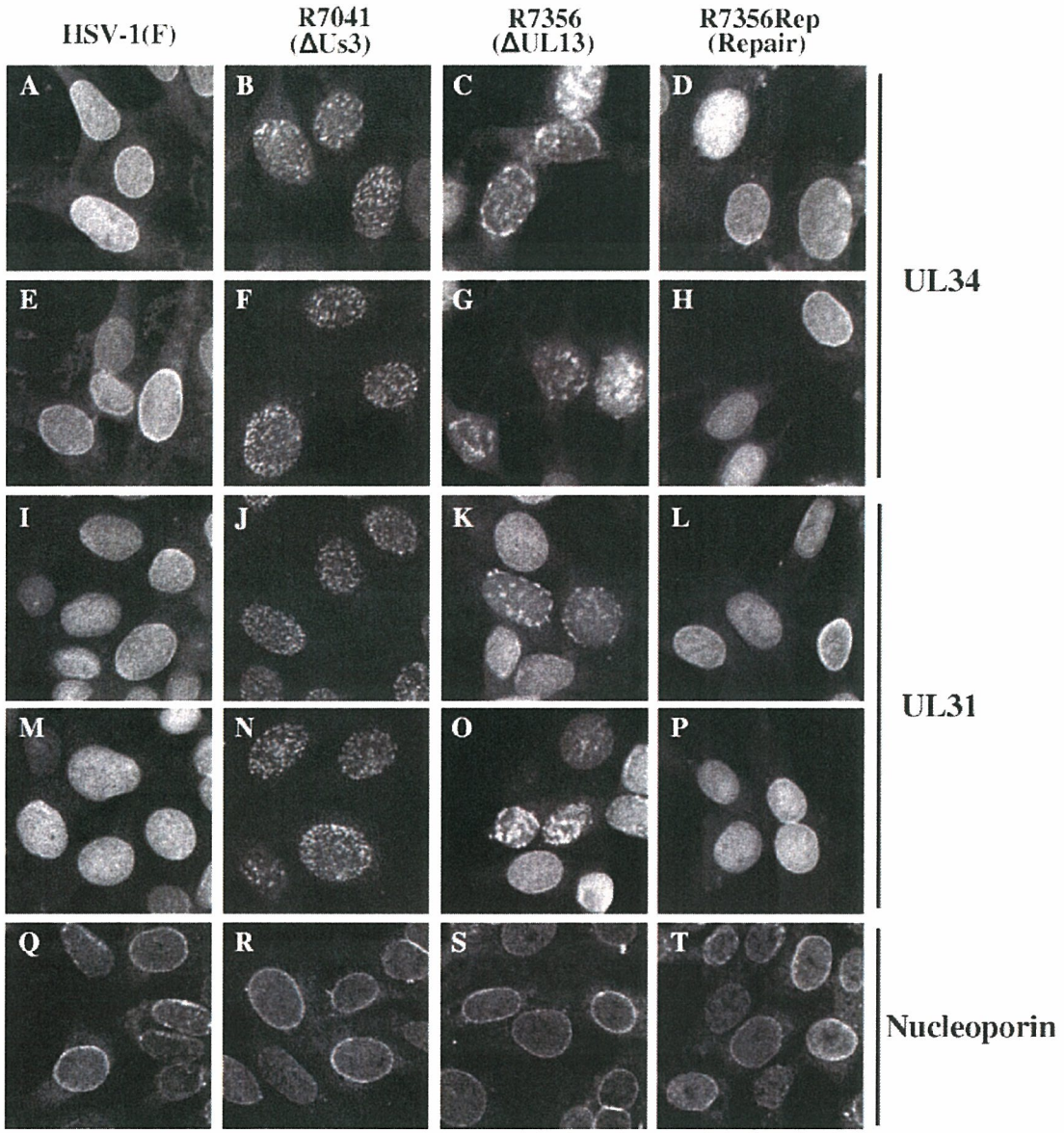

FIG. 5. Digital confocal microscope images showing localization of UL34, UL31, and nucleoporin p62 proteins in Vero cells infected with HSV-1(F) (A, E, I, M, and Q), R7041 (B, F, J, N, and R), R7356 (C, G, K, O, and S), and R7356Rep (D, H, L, P, and T). At 12 h postinfection, infected cells were fixed, permeabilized, and immunostained with rabbit polyclonal antibody to UL34 (A to H) detected with FITC-conjugated anti-rabbit IgG antibody, rabbit polyclonal antibody to UL31 (I to P) detected with Alexa Fluor 488-conjugated anti-rabbit IgG antibody, or mouse monoclonal antibody to nucleoporin p62 (Q to T) detected with Alexa Fluor 488-conjugated anti-mouse IgG antibody.

have on infected cells. The conclusions of these studies are as follows.

First, UL13 phosphorylates Us3 in vitro and in infected cells. Identification of the physiological substrate of a viral protein kinase requires demonstration that the substrate is specifically and directly phosphorylated by the kinase in vitro and that phosphorylation of the substrate in cells infected with a mutant virus lacking the protein kinase activity is altered. Although about 10 potential substrates of UL13 have been reported, only 3 (including gI/gE, ICP0, and EF-1δ) appear to fulfill the requirements to be natural UL13 substrates (4, 10, 20, 29, 32, 37, 44, 51, 57, 63). In the studies presented here, we have shown that a purified Us3 preparation was phosphorylated in vitro in the presence of purified recombinant UL13. The phosphorylation of Us3 was shown to be a direct effect of UL13 protein kinase activity and not of a contaminating kinase(s), because a kinase-negative mutant (GST-UL13K176M) was unable to phosphorylate Us3 in vitro. Furthermore, we found that Us3 phosphorylation was altered in cells infected with the UL13 deletion mutant virus. Thus, Us3 also fulfills the requirements to be a natural substrate of UL13 in infected cells.

Second, UL13 plays a role in the proper localization of UL34 and UL31 in infected cells. Previous studies have demonstrated that Us3 regulates the normal localization of the

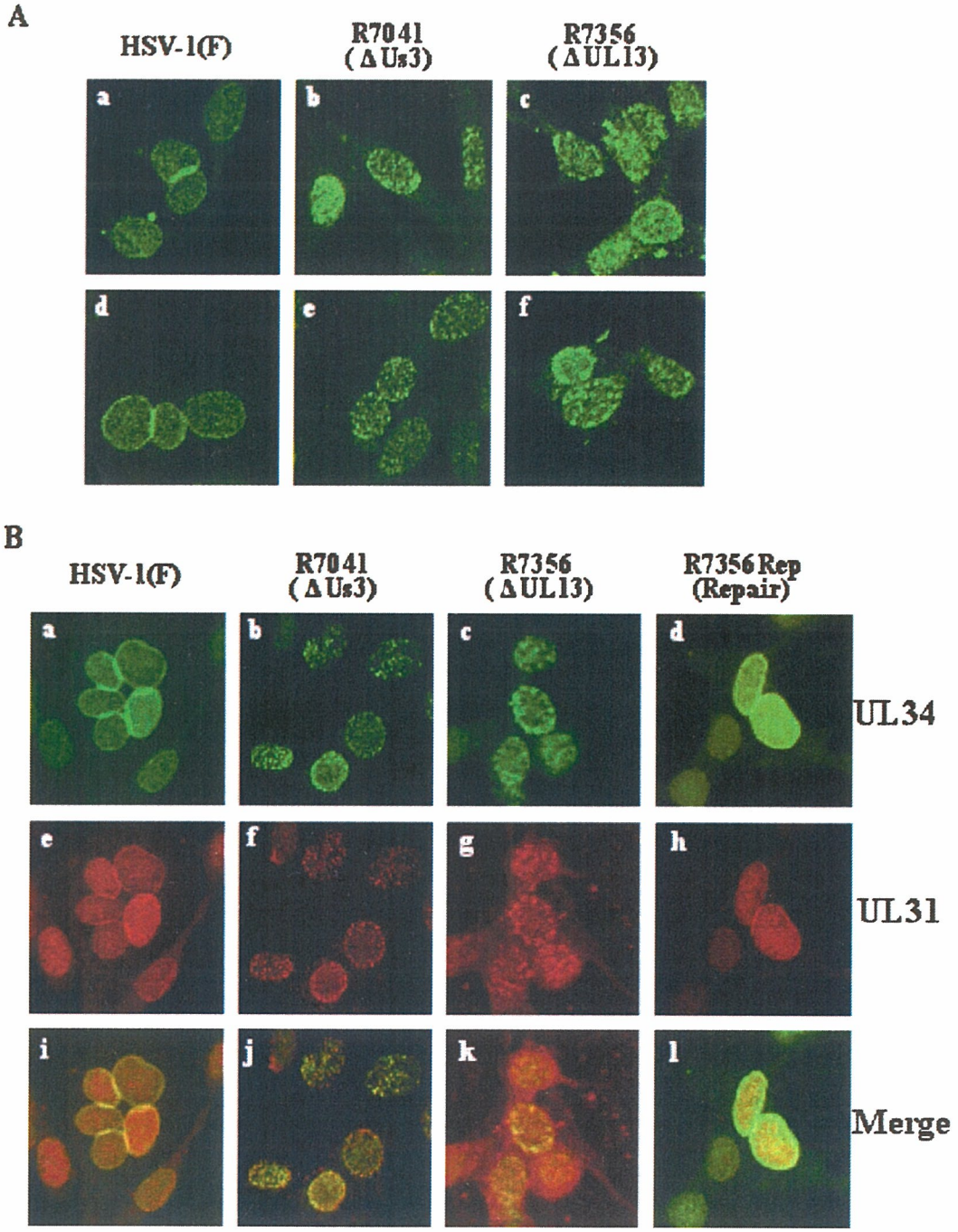

FIG. 6. (A) Digital confocal microscope images showing localization of UL34 in Vero cells infected with HSV-1(F) (a and d), R7041 (b and e), and R7356 (c and f). At 15 h postinfection, infected cells were fixed, permeabilized, and immunostained with rabbit polyclonal antibody to UL34 (a to c) detected with FITC-conjugated anti-rabbit IgG antibody or chicken polyclonal antibody to UL34 (d to f) detected with FITC-conjugated anti-chicken IgG antibody. (B) Digital confocal microscope images showing localization of UL34 and UL31 in Vero cells infected with HSV-1(F) (a, e, and i), R7041 (b, f, and j), R7356 (c, g, and k), and R7356Rep (d, h, and l). At 15 h postinfection, infected cells were fixed, permeabilized, and double labeled with a combination of chicken polyclonal antibody to UL34 (a to d) and rabbit polyclonal antibody to UL31 (e to h) and then detected with FITC-conjugated anti-chicken IgG antibody (green fluorescence) and Alexa-546-conjugated anti-rabbit IgG antibody (red fluorescence). Single-color images were captured separately and are shown in the upper (UL34) (a to d) and middle (UL31) (e to h) panels; the lower panels (i to l) represent simultaneous acquisitions of both colors. The yellow colors visualized in the merged images represent colocalization of UL34 and UL31.

HSV-1 envelopment factors UL34 and UL31, showing that these viral proteins are localized abnormally in punctate structures at the nuclear membrane in cells infected with recombinant viruses lacking a functional Us3 protein (61, 62, 65). In the studies reported here, we have shown that the phenotype of the UL13 deletion mutant virus with respect to UL34 and UL31 localization is similar to that of the Us3 deletion mutant. Together with the observation that UL13 phosphorylates Us3 in infected cells, a reasonable hypothesis is that UL13-mediated phosphorylation of Us3 may regulate the ability of Us3 to determine the proper localization of the viral proteins UL34 and UL31. Although we have shown here that UL13-mediated phosphorylation of Us3 is not required for optimal Us3 protein kinase activity, such phosphorylation might alter some other Us3 activity, such as substrate specificity or subcellular localization. Further studies will be needed to clarify whether UL13-mediated phosphorylation of Us3 is required for regulation of UL34 and UL31 localization. Such studies will need to include identification of the Us3 site(s) for UL13-mediated phosphorylation, construction of a recombinant virus with a mutated phosphorylaton site(s) in Us3, and investigation of the phenotype of this mutant virus with respect to UL34 and UL31 localization.

Alternatively, UL13 may regulate UL34 and UL31 localization independently of Us3. We previously reported that HSV-1 UL13 and its counterparts in other herpesviruses, including human cytomegalovirus UL97 and EBV BGLF4, and cellular protein kinase cdc2 phosphorylate the same amino acid residues on target proteins (27–29). In addition, Advani et al. have shown that HSV-1 infection activates cdc2 and that UL13 is required for this activation (1). It is well known that cdc2 modifies nuclear membranes by direct phosphorylation of nuclear envelope proteins (5, 46). In particular, phosphorylation of nuclear lamina and the lamin B receptor by cdc2 results in disassembly of nuclear lamina during mitosis (11, 16, 22, 38, 47, 48, 53, 72). Interestingly, both the UL34 and UL31 proteins have been reported to interact in vitro with lamin A/C, a major component of nuclear lamina, and to be required for HSV-mediated modification of lamin A/C and chromatin (60, 67). Therefore, UL13 may act like a cdc2 kinase or may activate cdc2 kinase to phosphorylate nuclear envelope proteins for proper targeting of UL34 and UL31 proteins at the nuclear membrane.

The possibility that UL13 directly phosphorylates UL34 and/or UL31 to regulate their localization seems less likely, based on the following observations. First, we have shown here that, in cells infected with UL13 deletion mutant virus, post-translational processing of UL31, which is associated with phosphorylation (25), could not be differentiated from that in cells infected with wild-type virus. Second, Ryckman and Roller (65) reported that UL34 phosphorylation was completely abolished in infected cells when the Us3 kinase target sites in UL34 (threonine 195 and serine 198) (25, 58, 65) were mutated, indicating that UL34 is phosphorylated only at threonine 195 and serine 198. There are no reports that UL13 and Us3 target the same substrate phosphorylation site(s).

In the present study, we have demonstrated that UL34 and UL31 exhibited nucleoplasmic localization, in addition to nuclear membrane localization. Although several laboratories have investigated the localization of UL34 and UL31, it remains enigmatic. Thus, some laboratories clearly demonstrated that UL34 and UL31 were detected only at the nuclear membrane in HSV-1-infected cells and in cells cotransfected with a UL34- and UL31-expressing plasmid (61, 62, 65). In contrast, the others, including this laboratory, reported nucleoplasmic localization of UL34 and/or UL31, in addition to nuclear membrane localization, in cells infected with HSV-1 or HSV-2 and in cells transiently coexpressing UL31 and UL34 (8, 66, 67, 73, 74). Furthermore, the nucleoplasmic distribution of pseudorabies virus UL31 and UL34 homologues in infected cells has also been reported (19). At present, we do not know how to explain these discrepancies. Although it has been reported that UL34 is a membrane-anchored protein (58, 59, 66), UL34 could also function as a nucleoplasmic protein. There is also a possibility that the methods for fixation of cells, staining conditions, and equipment used in immunofluorescence assays affect the detection of the viral proteins. Further studies will be needed to clarify this subject.

In conclusion, we have provided data showing that Us3 is a physiological substrate of UL13 and that UL13 regulates the localization of the HSV envelopment factors UL34 and UL31. Although direct linkage between UL13-mediated phosphorylation of Us3 and the regulatory effects of Us3 on UL34 and UL31 localization remains to be elucidated, our observations raise the interesting possibility that UL13 is also involved in the nuclear egress pathway of HSV-1. In agreement with this possibility, it has been reported that the ability of mutant human cytomegalovirus UL97 to bud through the nuclear membrane is severely impaired (35).

ACKNOWLEDGMENTS

We thank B. Roizman for R7356, R7041, pBC1013, pBC1015, and SK-N-SH cells and R. Roller for chicken polyclonal antibody to UL34. We thank H. Noma for excellent technical assistance.

This study was supported in part by Grants for Scientific Research and Grants for Scientific Research in Priority Areas from the Ministry of Education, Science, Sports and Culture of Japan.

REFERENCES

1. **Advani, S. J., R. Brandimarti, R. R. Weichselbaum, and B. Roizman.** 2000. The disappearance of cyclins A and B and the increase in activity of the G_2/M-phase cellular kinase cdc2 in herpes simplex virus 1-infected cells require expression of the alpha22/U(S)1.5 and U(L)13 viral genes. J. Virol. **74**:8–15.
2. **Asano, S., T. Honda, F. Goshima, D. Watanabe, Y. Miyake, Y. Sugiura, and Y. Nishiyama.** 1999. US3 protein kinase of herpes simplex virus type 2 plays a role in protecting corneal epithelial cells from apoptosis in infected mice. J. Gen. Virol. **80**:51–56.
3. **Benetti, L., and B. Roizman.** 2004. Herpes simplex virus protein kinase US3 activates and functionally overlaps protein kinase A to block apoptosis. Proc. Natl. Acad. Sci. USA **101**:9411–9416.
4. **Bruni, R., B. Fineschi, W. O. Ogle, and B. Roizman.** 1999. A novel cellular protein, p60, interacting with both herpes simplex virus 1 regulatory proteins ICP22 and ICP0 is modified in a cell-type-specific manner and is recruited to the nucleus after infection. J. Virol. **73**:3810–3817.
5. **Buendia, B., J. C. Courvalin, and P. Collas.** 2001. Dynamics of the nuclear envelope at mitosis and during apoptosis. Cell Mol. Life Sci. **58**:1781–1789.
6. **Cartier, A., E. Broberg, T. Komai, M. Henriksson, and M. G. Masucci.** 2003. The herpes simplex virus-1 Us3 protein kinase blocks CD8T cell lysis by preventing the cleavage of Bid by granzyme B. Cell Death Differ. **10**:1320–1328.
7. **Cartier, A., T. Komai, and M. G. Masucci.** 2003. The Us3 protein kinase of herpes simplex virus 1 blocks apoptosis and induces phosporylation of the Bcl-2 family member Bad. Exp. Cell Res. **291**:242–250.
8. **Chang, Y. E., and B. Roizman.** 1993. The product of the UL31 gene of herpes simplex virus 1 is a nuclear phosphoprotein which partitions with the nuclear matrix. J. Virol. **67**:6348–6356.
9. **Chee, M. S., G. L. Lawrence, and B. G. Barrell.** 1989. Alpha-, beta- and gammaherpesviruses encode a putative phosphotransferase. J. Gen. Virol. **70**:1151–1160.

10. **Coulter, L. J., H. W. Moss, J. Lang, and D. J. McGeoch.** 1993. A mutant of herpes simplex virus type 1 in which the UL13 protein kinase gene is disrupted. J. Gen. Virol. **74:**387–395.
11. **Courvalin, J. C., N. Segil, G. Blobel, and H. J. Worman.** 1992. The lamin B receptor of the inner nuclear membrane undergoes mitosis-specific phosphorylation and is a substrate for p34cdc2-type protein kinase. J. Biol. Chem. **267:**19035–19038.
12. **Cunningham, C., A. J. Davison, A. Dolan, M. C. Frame, D. J. McGeoch, D. M. Meredith, H. W. Moss, and A. C. Orr.** 1992. The UL13 virion protein of herpes simplex virus type 1 is phosphorylated by a novel virus-induced protein kinase. J. Gen. Virol. **73:**303–311.
13. **Daikoku, T., S. Shibata, F. Goshima, S. Oshima, T. Tsurumi, H. Yamada, Y. Yamashita, and Y. Nishiyama.** 1997. Purification and characterization of the protein kinase encoded by the UL13 gene of herpes simplex virus type 2. Virology **235:**82–93.
14. **Daikoku, T., Y. Yamashita, T. Tsurumi, K. Maeno, and Y. Nishiyama.** 1993. Purification and biochemical characterization of the protein kinase encoded by the US3 gene of herpes simplex virus type 2. Virology **197:**685–694.
15. **Dancey, J. E.** 2004. Molecular targeting: PI3 kinase pathway. Ann. Oncol. **15**(Suppl. 4):iv233–iv239.
16. **Dessev, G., C. Iovcheva-Dessev, J. R. Bischoff, D. Beach, and R. Goldman.** 1991. A complex containing p34cdc2 and cyclin B phosphorylates the nuclear lamin and disassembles nuclei of clam oocytes in vitro. J. Cell Biol. **112:**523–533.
17. **Ejercito, P. M., E. D. Kieff, and B. Roizman.** 1968. Characterization of herpes simplex virus strains differing in their effects on social behaviour of infected cells. J. Gen. Virol. **2:**357–364.
18. **Frame, M. C., F. C. Purves, D. J. McGeoch, H. S. Marsden, and D. P. Leader.** 1987. Identification of the herpes simplex virus protein kinase as the product of viral gene US3. J. Gen. Virol. **68:**2699–2704.
19. **Fuchs, W., B. G. Klupp, H. Granzow, N. Osterrieder, and T. C. Mettenleiter.** 2002. The interacting UL31 and UL34 gene products of pseudorabies virus are involved in egress from the host-cell nucleus and represent components of primary enveloped but not mature virions. J. Virol. **76:**364–378.
20. **Geiss, B. J., J. E. Tavis, L. M. Metzger, D. A. Leib, and L. A. Morrison.** 2001. Temporal regulation of herpes simplex virus type 2 VP22 expression and phosphorylation. J. Virol. **75:**10721–10729.
21. **Goshima, F., T. Daikoku, H. Yamada, S. Oshima, T. Tsurumi, and Y. Nishiyama.** 1998. Subcellular localization of the US3 protein kinase of herpes simplex virus type 2. Arch. Virol. **143:**613–622.
22. **Heald, R., and F. McKeon.** 1990. Mutations of phosphorylation sites in lamin A that prevent nuclear lamina disassembly in mitosis. Cell **61:**579–589.
23. **Jerome, K. R., R. Fox, Z. Chen, A. E. Sears, H. Lee, and L. Corey.** 1999. Herpes simplex virus inhibits apoptosis through the action of two genes, Us5 and Us3. J. Virol. **73:**8950–8957.
24. **Kanamori, M., S. Watanabe, R. Honma, M. Kuroda, S. Imai, K. Takada, N. Yamamoto, Y. Nishiyama, and Y. Kawaguchi.** 2004. Epstein-Barr virus nuclear antigen leader protein induces expression of thymus- and activation-regulated chemokine in B cells. J. Virol. **78:**3984–3993.
25. **Kato, A., M. Yamamoto, T. Ohno, H. Kodaira, Y. Nishiyama, and Y. Kawaguchi.** 2005. Identification of proteins phosphorylated directly by the Us3 protein kinase encoded by herpes simplex virus 1. J. Virol. **79:**9325–9331.
26. **Kato, K., Y. Kawaguchi, M. Tanaka, M. Igarashi, A. Yokoyama, G. Matsuda, M. Kanamori, K. Nakajima, Y. Nishimura, M. Shimojima, H. T. Phung, E. Takahashi, and K. Hirai.** 2001. Epstein-Barr virus-encoded protein kinase BGLF4 mediates hyperphosphorylation of cellular elongation factor 1δ (EF-1δ): EF-1δ is universally modified by conserved protein kinases of herpesviruses in mammalian cells. J. Gen. Virol. **82:**1457–1463.
27. **Kato, K., A. Yokoyama, Y. Tohya, H. Akashi, Y. Nishiyama, and Y. Kawaguchi.** 2003. Identification of protein kinases responsible for phosphorylation of Epstein-Barr virus nuclear antigen leader protein at serine-35, which regulates its coactivator function. J. Gen. Virol. **84:**3381–3392.
28. **Kawaguchi, Y., and K. Kato.** 2003. Protein kinases conserved in herpesviruses potentially share a function mimicking the cellular protein kinase cdc2. Rev. Med. Virol. **13:**331–340.
29. **Kawaguchi, Y., K. Kato, M. Tanaka, M. Kanamori, Y. Nishiyama, and Y. Yamanashi.** 2003. Conserved protein kinases encoded by herpesviruses and cellular protein kinase cdc2 target the same phosphorylation site in eukaryotic elongation factor 1δ. J. Virol. **77:**2359–2368.
30. **Kawaguchi, Y., T. Matsumura, B. Roizman, and K. Hirai.** 1999. Cellular elongation factor 1δ is modified in cells infected with representative alpha-, beta-, or gammaherpesviruses. J. Virol. **73:**4456–4460.
31. **Kawaguchi, Y., K. Nakajima, M. Igarashi, T. Morita, M. Tanaka, M. Suzuki, A. Yokoyama, G. Matsuda, K. Kato, M. Kanamori, and K. Hirai.** 2000. Interaction of Epstein-Barr virus nuclear antigen leader protein (EBNA-LP) with HS1-associated protein X-1: implication of cytoplasmic function of EBNA-LP. J. Virol. **74:**10104–10111.
32. **Kawaguchi, Y., C. Van Sant, and B. Roizman.** 1998. Eukaryotic elongation factor 1δ is hyperphosphorylated by the protein kinase encoded by the U(L)13 gene of herpes simplex virus 1. J. Virol. **72:**1731–1736.
33. **Kawaguchi, Y., C. Van Sant, and B. Roizman.** 1997. Herpes simplex virus 1 alpha regulatory protein ICP0 interacts with and stabilizes the cell cycle regulator cyclin D3. J. Virol. **71:**7328–7336.
34. **Klupp, B. G., H. Granzow, and T. C. Mettenleiter.** 2001. Effect of the pseudorabies virus US3 protein on nuclear membrane localization of the UL34 protein and virus egress from the nucleus. J. Gen. Virol. **82:**2363–2371.
35. **Krosky, P. M., M. C. Baek, and D. M. Coen.** 2003. The human cytomegalovirus UL97 protein kinase, an antiviral drug target, is required at the stage of nuclear egress. J. Virol. **77:**905–914.
36. **Leopardi, R., C. Van Sant, and B. Roizman.** 1997. The herpes simplex virus 1 protein kinase US3 is required for protection from apoptosis induced by the virus. Proc. Natl. Acad. Sci. USA **94:**7891–7896.
37. **Long, M. C., V. Leong, P. A. Schaffer, C. A. Spencer, and S. A. Rice.** 1999. ICP22 and the UL13 protein kinase are both required for herpes simplex virus-induced modification of the large subunit of RNA polymerase II. J. Virol. **73:**5593–5604.
38. **Luscher, B., L. Brizuela, D. Beach, and R. N. Eisenman.** 1991. A role for the p34cdc2 kinase and phosphatases in the regulation of phosphorylation and disassembly of lamin B2 during the cell cycle. EMBO J. **10:**865–875.
39. **McGeoch, D. J., and A. J. Davison.** 1986. Alphaherpesviruses possess a gene homologous to the protein kinase gene family of eukaryotes and retroviruses. Nucleic Acids Res. **14:**1765–1777.
40. **Morrison, E. E., Y. F. Wang, and D. M. Meredith.** 1998. Phosphorylation of structural components promotes dissociation of the herpes simplex virus type 1 tegument. J. Virol. **72:**7108–7114.
41. **Munger, J., A. V. Chee, and B. Roizman.** 2001. The U(S)3 protein kinase blocks apoptosis induced by the d120 mutant of herpes simplex virus 1 at a premitochondrial stage. J. Virol. **75:**5491–5497.
42. **Munger, J., and B. Roizman.** 2001. The US3 protein kinase of herpes simplex virus 1 mediates the posttranslational modification of BAD and prevents BAD-induced programmed cell death in the absence of other viral proteins. Proc. Natl. Acad. Sci. USA **98:**10410–10415.
43. **Murata, T., F. Goshima, Y. Yamauchi, T. Koshizuka, H. Takakuwa, and Y. Nishiyama.** 2002. Herpes simplex virus type 2 US3 blocks apoptosis induced by sorbitol treatment. Microbes Infect. **4:**707–712.
44. **Ng, T. I., W. O. Ogle, and B. Roizman.** 1998. UL13 protein kinase of herpes simplex virus 1 complexes with glycoprotein E and mediates the phosphorylation of the viral Fc receptor: glycoproteins E and I. Virology **241:**37–48.
45. **Ng, T. I., C. Talarico, T. C. Burnette, K. Biron, and B. Roizman.** 1996. Partial substitution of the functions of the herpes simplex virus 1 U(L)13 gene by the human cytomegalovirus U(L)97 gene. Virology **225:**347–358.
46. **Nigg, E. A.** 1993. Cellular substrates of p34cdc2 and its companion cyclin-dependent kinases. Trends Cell Biol. **3:**296–301.
47. **Nikolakaki, E., J. Meier, G. Simos, S. D. Georgatos, and T. Giannakouros.** 1997. Mitotic phosphorylation of the lamin B receptor by a serine/arginine kinase and p34(cdc2). J. Biol. Chem. **272:**6208–6213.
48. **Nikolakaki, E., G. Simos, S. D. Georgatos, and T. Giannakouros.** 1996. A nuclear envelope-associated kinase phosphorylates arginine-serine motifs and modulates interactions between the lamin B receptor and other nuclear proteins. J. Biol. Chem. **271:**8365–8372.
49. **Nishiyama, Y., Y. Yamada, R. Kurachi, and T. Daikoku.** 1992. Construction of a US3 *lacZ* insertion mutant of herpes simplex virus type 2 and characterization of its phenotype in vitro and in vivo. Virology **190:**256–268.
50. **Ogg, P. D., P. J. McDonell, B. J. Ryckman, C. M. Knudson, and R. J. Roller.** 2004. The HSV-1 Us3 protein kinase is sufficient to block apoptosis induced by overexpression of a variety of Bcl-2 family members. Virology **319:**212–224.
51. **Ogle, W. O., T. I. Ng, K. L. Carter, and B. Roizman.** 1997. The UL13 protein kinase and the infected cell type are determinants of posttranslational modification of ICP0. Virology **235:**406–413.
52. **Overton, H. A., D. J. McMillan, L. S. Klavinskis, L. Hope, A. J. Ritchie, and P. Wong-Kai-In.** 1992. Herpes simplex virus type 1 gene UL13 encodes a phosphoprotein that is a component of the virion. Virology **190:**184–192.
53. **Peter, M., J. Nakagawa, M. Doree, J. C. Labbe, and E. A. Nigg.** 1990. In vitro disassembly of the nuclear lamina and M phase-specific phosphorylation of lamins by cdc2 kinase. Cell **61:**591–602.
54. **Poon, A. P., and B. Roizman.** 2005. Herpes simplex virus 1 ICP22 regulates the accumulation of a shorter mRNA and of a truncated US3 protein kinase that exhibits altered functions. J. Virol. **79:**8470–8479.
55. **Purves, F. C., R. M. Longnecker, D. P. Leader, and B. Roizman.** 1987. Herpes simplex virus 1 protein kinase is encoded by open reading frame US3 which is not essential for virus growth in cell culture. J. Virol. **61:**2896–2901.
56. **Purves, F. C., W. O. Ogle, and B. Roizman.** 1993. Processing of the herpes simplex virus regulatory protein alpha 22 mediated by the UL13 protein kinase determines the accumulation of a subset of alpha and gamma mRNAs and proteins in infected cells. Proc. Natl. Acad. Sci. USA **90:**6701–6705.
57. **Purves, F. C., and B. Roizman.** 1992. The UL13 gene of herpes simplex virus 1 encodes the functions for posttranslational processing associated with phosphorylation of the regulatory protein alpha 22. Proc. Natl. Acad. Sci. USA **89:**7310–7314.
58. **Purves, F. C., D. Spector, and B. Roizman.** 1991. The herpes simplex virus 1 protein kinase encoded by the US3 gene mediates posttranslational modifi-

cation of the phosphoprotein encoded by the UL34 gene. J. Virol. **65:**5757–5764.

59. **Purves, F. C., D. Spector, and B. Roizman.** 1992. UL34, the target of the herpes simplex virus U(S)3 protein kinase, is a membrane protein which in its unphosphorylated state associates with novel phosphoproteins. J. Virol. **66:**4295–4303.
60. **Reynolds, A. E., L. Liang, and J. D. Baines.** 2004. Conformational changes in the nuclear lamina induced by herpes simplex virus type 1 require genes U(L)31 and U(L)34. J. Virol. **78:**5564–5575.
61. **Reynolds, A. E., B. J. Ryckman, J. D. Baines, Y. Zhou, L. Liang, and R. J. Roller.** 2001. U(L)31 and U(L)34 proteins of herpes simplex virus type 1 form a complex that accumulates at the nuclear rim and is required for envelopment of nucleocapsids. J. Virol. **75:**8803–8817.
62. **Reynolds, A. E., E. G. Wills, R. J. Roller, B. J. Ryckman, and J. D. Baines.** 2002. Ultrastructural localization of the herpes simplex virus type 1 UL31, UL34, and US3 proteins suggests specific roles in primary envelopment and egress of nucleocapsids. J. Virol. **76:**8939–8952.
63. **Roizman, B., and D. M. Knipe.** 2001. Herpes simplex viruses and their replication, p. 2399–2459. *In* D. M. Knipe, P. M. Howley, D. E. Griffin, R. A. Lamb, M. A. Martin, B. Roizman, and S. E. Straus (ed.), Fields virology, 4th ed. Lippincott-Williams &Wilkins, Philadelphia, Pa.
64. **Roller, R. J., Y. Zhou, R. Schnetzer, J. Ferguson, and D. DeSalvo.** 2000. Herpes simplex virus type 1 U(L)34 gene product is required for viral envelopment. J. Virol. **74:**117–129.
65. **Ryckman, B. J., and R. J. Roller.** 2004. Herpes simplex virus type 1 primary envelopment: UL34 protein modification and the US3-UL34 catalytic relationship. J. Virol. **78:**399–412.
66. **Shiba, C., T. Daikoku, F. Goshima, H. Takakuwa, Y. Yamauchi, O. Koiwai, and Y. Nishiyama.** 2000. The UL34 gene product of herpes simplex virus type 2 is a tail-anchored type II membrane protein that is significant for virus envelopment. J. Gen. Virol. **81:**2397–2405.
67. **Simpson-Holley, M., J. Baines, R. Roller, and D. M. Knipe.** 2004. Herpes simplex virus 1 U(L)31 and U(L)34 gene products promote the late maturation of viral replication compartments to the nuclear periphery. J. Virol. **78:**5591–5600.
68. **Smith, R. F., and T. F. Smith.** 1989. Identification of new protein kinase-related genes in three herpesviruses, herpes simplex virus, varicella-zoster virus, and Epstein-Barr virus. J. Virol. **63:**450–455.
69. **Tanaka, M., H. Kagawa, Y. Yamanashi, T. Sata, and Y. Kawaguchi.** 2003. Construction of an excisable bacterial artificial chromosome containing a full-length infectious clone of herpes simplex virus type 1: viruses reconstituted from the clone exhibit wild-type properties in vitro and in vivo. J. Virol. **77:**1382–1391.
70. **Tanaka, M., Y. Nishiyama, T. Sata, and Y. Kawaguchi.** 2005. The role of protein kinase activity expressed by the UL13 gene of herpes simplex virus 1: the activity is not essential for optimal expression of UL41 and ICP0. Virology **341:**301–312.
71. **Wagenaar, F., J. M. Pol, B. Peeters, A. L. Gielkens, N. de Wind, and T. G. Kimman.** 1995. The US3-encoded protein kinase from pseudorabies virus affects egress of virions from the nucleus. J Gen. Virol. **76:**1851–1859.
72. **Ward, G. E., and M. W. Kirschner.** 1990. Identification of cell cycle-regulated phosphorylation sites on nuclear lamin C. Cell **61:**561–577.
73. **Yamada, H., Y. M. Jiang, S. Oshima, T. Daikoku, Y. Yamashita, T. Tsurumi, and Y. Nishiyama.** 1998. Characterization of the UL55 gene product of herpes simplex virus type 2. J. Gen. Virol. **79:**1989–1995.
74. **Yamauchi, Y., C. Shiba, F. Goshima, A. Nawa, T. Murata, and Y. Nishiyama.** 2001. Herpes simplex virus type 2 UL34 protein requires UL31 protein for its relocation to the internal nuclear membrane in transfected cells. J. Gen. Virol. **82:**1423–1428.
75. **Yokoyama, A., M. Tanaka, G. Matsuda, K. Kato, M. Kanamori, H. Kawasaki, H. Hirano, I. Kitabayashi, M. Ohki, K. Hirai, and Y. Kawaguchi.** 2001. Identification of major phosphorylation sites of Epstein-Barr virus nuclear antigen leader protein (EBNA-LP): ability of EBNA-LP to induce latent membrane protein 1 cooperatively with EBNA-2 is regulated by phosphorylation. J. Virol. **75:**5119–5128.
76. **Yue, W., E. Gershburg, and J. S. Pagano.** 2005. Hyperphosphorylation of EBNA2 by Epstein-Barr virus protein kinase suppresses transactivation of the LMP1 promoter. J. Virol. **79:**5880–5885.
77. **Zarubin, T., and J. Han.** 2005. Activation and signaling of the p38 MAP kinase pathway. Cell Res. **15:**11–18.
78. **Zhu, H. Y., H. Yamada, Y. M. Jiang, M. Yamada, and Y. Nishiyama.** 1999. Intracellular localization of the UL31 protein of herpes simplex virus type 2. Arch. Virol. **144:**1923–1935.

Available online at www.sciencedirect.com
SCIENCE DIRECT
Microbes and Infection 8 (2006) 1054–1063
Microbes and Infection
www.elsevier.com/locate/micinf

Original article

Construction of an infectious clone of canine herpesvirus genome as a bacterial artificial chromosome

Jun Arii [a,1], Orkash Hushur [a,1], Kentaro Kato [a], Yasushi Kawaguchi [b,c], Yukinobu Tohya [a,*], Hiroomi Akashi [a]

[a] *Department of Veterinary Microbiology, Graduate School of Agricultural and Life Sciences, The University of Tokyo, 1-1-1, Yayoi, Bunkyo-ku, Tokyo 113-8657, Japan*
[b] *Department of Virology, Graduate School of Medicine, Nagoya University, 65 Showa-ku, Nagoya 466-8550, Japan*
[c] *PRESTO, Japan Science and Technology Agency, Honcho 4-1-8, Kawaguchi, Saitama 332-0012, Japan*

Received 30 June 2005; accepted 31 October 2005
Available online 19 January 2006

Abstract

Canine herpesvirus (CHV) is an attractive candidate not only for use as a recombinant vaccine to protect dogs from a variety of canine pathogens but also as a viral vector for gene therapy in domestic animals. However, developments in this area have been impeded by the complicated techniques used for eukaryotic homologous recombination. To overcome these problems, we used bacterial artificial chromosomes (BACs) to generate infectious BACs. Our findings may be summarized as follows: (i) the CHV genome (pCHV/BAC), in which a BAC flanked by loxP sites was inserted into the thymidine kinase gene, was maintained in *Escherichia coli*; (ii) transfection of pCHV/BAC into A-72 cells resulted in the production of infectious virus; (iii) the BAC vector sequence was almost perfectly excisable from the genome of the reconstituted virus CHV/BAC by co-infection with CHV/BAC and a recombinant adenovirus that expressed the Cre recombinase; and (iv) a recombinant virus in which the glycoprotein C gene was deleted was generated by λ recombination followed by Flp recombination, which resulted in a reduction in viral titer compared with that of the wild-type virus. The infectious clone pCHV/BAC is useful for the modification of the CHV genome using bacterial genetics, and CHV/BAC should have multiple applications in the rapid generation of genetically engineered CHV recombinants and the development of CHV vectors for vaccination and gene therapy in domestic animals.

Keywords: Bacterial artificial chromosome; Canine herpesvirus; Flp recombination

1. Introduction

Canine herpesvirus (CHV) is a member of the Alphaherpesvirinae subfamily of the Herpesviridae [1]. Since the clinical signs of CHV infection of adult dogs are usually mild or undetectable, it is not considered to be a serious pathogen of dogs. However, CHV is the etiological agent of severe illness of puppies of less than 2 weeks of age, causing a generalized necrotizing and hemorrhagic disease, which is usually fatal [2]. CHV is also transmitted transplacentally, resulting in fetal death [3]. Although surveys have shown a relatively high prevalence of CHV in household and colony-bred dogs [4,5], CHV is known to be associated with fertility disorders, which are limited in breeding dogs. Due to its low inherent virulence, CHV is an attractive candidate not only for use as an attenuated vector and a recombinant vaccine to protect dogs from CHV and a variety of canine pathogens [6] but also for gene therapy of domestic dogs. As the host range of CHV is limited to dogs [2], the CHV vector can be used safely in other species, such as humans.

Abbreviations: CHV, canine herpesvirus; BAC, bacterial artificial chromosome; gC, glycoprotein C; GFP, green fluorescent protein; TK, thymidine kinase.

* Corresponding author. Tel.: +81 3 5841 5397; fax: +81 3 5841 8184.
E-mail address: aytohya@mail.ecc.u-tokyo.ac.jp (Y. Tohya).

[1] J. A. and O. H. contributed equally to this work.

1286-4579/$ - see front matter © 2005 Elsevier SAS. All rights reserved.
doi:10.1016/j.micinf.2005.11.004

The gene structure of CHV has yet to be determined, since no CHV strain has been completely sequenced and only a few genes have been identified [6,7]. Restriction mapping and partial determination of nucleotide sequences have shown that the overall structure of CHV resembles those of other alphaherpesviruses [8]. The availability of virus mutants and gene deletions would contribute significantly to the production of CHV-based attenuated or recombinant vaccines, potentially CHV-based gene therapies for domestic animals. Although a CHV vaccine is not currently available clinically, a few reports regarding the development of recombinant CHV constructs have been published [8–12]. All of the recombinant CHVs reported to date have been produced utilizing conventional techniques that are based on eukaryotic homologous recombination, which is technically difficult and time-consuming due to the requirement of multiple rounds of purification of recombinant viruses. None of these approaches has fully exploited the potential of CHV as a vector.

Recently, manipulations of the large herpesvirus genomes have been made using bacterial artificial chromosomes (BACs) [13]. Using this method, any genetic modification of the herpesvirus genome can be introduced quickly in *Escherichia coli* (*E. coli*) and generated efficiently without further plaque purification in eukaryotic cells [14]. To date, the genomes of several animal and human herpesviruses have been successfully propagated as infectious BAC clones [14–29].

In this study, we attempted to generate an infectious CHV/BAC clone in which the BAC vector is inserted into the thymidine kinase (TK) gene. The salient features of the CHV/BAC produced in this way are: (i) the BAC vector sequence is efficiently removed by a Cre/loxP site-specific recombination system using a recombinant adenovirus that expresses the Cre recombinase; (ii) the manipulation of the BAC-cloned CHV infectious genome was confirmed by deletion of the glycoprotein C (gC) gene by λ recombination followed by Flp recombination; and (iii) this study is the first to describe the construction of a herpesvirus cloned as an infectious BAC, with the aim of exploitation in the vaccination and gene therapy of companion animals in the future.

2. Materials and methods

2.1. Cells and viruses

Madin–Darby canine kidney (MDCK) cells [30] and A-72 cells [31] were cultured in Dulbecco's modified Eagle's medium (DMEM; Nissui, Tokyo, Japan) that was supplemented with 5% heat-inactivated fetal calf serum (FCS), penicillin, and streptomycin. The CHV DFD-6 strain [32] was used in this study. A recombinant adenovirus AxCANCre [33] was propagated, and titrated in 293 cells according to the instructions of the manufacturer (TaKaRa, Otsu, Japan).

2.2. Plasmids and vectors

p246MCS, which contains two loxP sites in direct orientation to each other, was constructed as follows. The 30-bp *Bam*HI–*Hin*dIII fragment of pBeloBAC11 (Research Genetics) multi-cloning site (MCS) was cloned into pBS246 (Gibco, Carlsbad, CA) by digestion with *Bam*HI–*Hin*dIII to replace the MCS between the two loxP sites with the MCS of pBeloBAC11, thereby generating p246MCS. p246dBGFP, which contains the green fluorescent protein (GFP) expression cassette flanked by two loxP sites in direct orientation to each other, was constructed as follows. The 1.6-kb *Ase*I–*Mlu*I fragment that contains the GFP expression cassette derived from pEGFP-C1 (Clontech, Franklin Lakes, NJ), of which the *Bgl*II–*Bam*HI fragment in the MCS had been deleted, was blunt-ended by Klenow (TaKaRa) and cloned into the *Bam*HI site of p246MCS, resulting in p246dBGFP.

pCTK, which contains the CHV TK gene and flanking region for homologous recombination, was constructed as follows. The 6-kb TK-flanking region, which includes the TK gene, was amplified from purified CHV genomic DNA by the polymerase chain reaction (PCR) using standard procedures with the following primers: 5′-gacctcgagcatacctaaactacctgg-3′, which contains an *Xho*I site at the 5′-end; and 5′-acactgcaggtgatgagaggggcttatt-3′, which contains a *Pst*I site at the 5′-end. The PCR product was digested with *Pst*I and *Xho*I, and cloned into the *Pst*I–*Xho*I sites of pBluescript II KS(+) (Stratagene, La Jolla, CA), thereby generating pCTK. The transfer vector pCTKdEHGFP, which contains the *Eco*RI–*Hin*dIII-deleted TK gene, TK-flanking region, and a GFP expression cassette between two loxP sites, was constructed by ligation of the *Eco*RI–*Spe*I fragment, which contains the GFP expression cassette derived from p246dBGFP, into *Eco*RI–*Hin*dIII-digested pCTK. The resultant linear fragment, in which the protruding end generated by *Spe*I still remained, was blunt-ended by Klenow and self-ligated. The BAC vector pBeloBAC11 was digested with *Sal*I, purified, and ligated into pCTKdEHGFP, which had been digested with *Sal*I and dephosphorylated. All of the constructs were transformed into the *E. coli* strain XL-1 Blue strain. The transformants were plated on selective agar that contained 100 μg/ml ampicillin and/or 12.5 μg/ml chloramphenicol (Cm).

2.3. Virus construction

CHV/BAC was constructed as follows. Confluent MDCK monolayers were transfected with pCTKdEHBAC using Lipofectamine 2000 (Invitrogen, Carlsbad, CA) according to the manufacturer's instruction. Briefly, for each transfection, 2 μg of linear *Not*I-digested vector pCTKdEHBAC and 10 μl of Lipofectamine were diluted separately in 250 μl of Opti-MEM (Gibco) in two tubes and incubated at room temperature for 15 min. Then, the two dilutions were mixed and further incubated at room temperature for 20 min to allow the formation of lipid–DNA complexes. This reaction mixture was added to monolayers cultivated in a six-well plate (Corning, New York, NY), in which the growth medium had been replaced with maintenance medium (DMEM that contained 1% FCS) and incubated at 37 °C with 5% CO_2 for 24 h. Then, the cells were infected with approximately 100 plaque-forming units (PFU) of CHV and incubated for 3 days. The diluted virus pool

was incubated with MDCK cells for 3 days in maintenance medium. The progeny viruses (called CHV/BAC) were plaque-purified based on the expression of GFP.

2.4. Isolation and transformation of viral DNAs

CHV nucleocapsid DNA was isolated according to the methods developed by Sinzger et al. [34]. In brief, infected cells were harvested when all the cells showed the cytopathic effect (CPE), collected by low-speed centrifugation, and washed twice with cold phosphate-buffered saline (PBS). The cells were resuspended in cell permeabilization buffer [10 mM Tris–HCl (pH 7.5), 320 mM $MgCl_2$, 1% Triton X-100], incubated on ice for 10 min, and then treated with micrococcal nuclease (1500 U/ml; Amersham Biosciences, Piscataway, NJ) at 37 °C for 60 min. After nuclease treatment, the cells were digested with 100 μg/ml proteinase K (Invitrogen) at 50 °C overnight, and viral DNA was extracted with phenol–chloroform and precipitated with isopropanol. Circular viral DNA was isolated by the method of Hirt [35]. Briefly, confluent MDCK cells in a 60-mm tissue culture dish (Corning) were infected with 3 PFU CHV/BAC per cell, incubated for 7 h, harvested, washed once with PBS, and lysed in 0.4 ml of buffer A (0.6% SDS, 10 mM EDTA) for 30 min at room temperature. Then, 0.1 ml of 5 M NaCl was added, and after incubation of the cell lysate at 4 °C for 24 h, the cell debris was clarified by centrifugation. The supernatant was extracted twice with phenol–chloroform and the DNA was precipitated with ethanol. For cloning of the CHV/BAC genome, replicative intermediate (covalently closed circular) CHV/BAC DNA was isolated and transformed into *E. coli* DH10B (Invitrogen) by electroporation using the ECM 830 Pulse Generator (Genetronics, San Diego, CA) with 0.1-cm cuvettes and pulsing at 2.4 kV for 99 μs. The transformed cells were grown on LB plates that contained 12.5 μg/ml of Cm. BAC DNA samples were isolated from the *E. coli* cultures by standard alkaline lysis procedures [36] and the construct was designated as pCHV/BAC.

2.5. Reconstitution of infectious virus from BAC

A-72 cells were seeded on six-well plates at 5×10^5 cells/well 24 h prior to transfection and incubated at 37 °C in the atmosphere of 5% CO_2. Transfection of pCHV/BAC DNA into the A-72 monolayer was performed using TransIT-LT1 (Mirus, Madison, WI), as described below. For each transfection, 12 μl of TransIT-LT1 reagent was diluted in 500 μl Opti-MEM. Following a 15-min incubation at room temperature, 2 μg of pCHV/BAC DNA was added and the cells were incubated at room temperature for 15 min. The resultant reaction mixture was added to the monolayer, for which the growth medium had been exchanged with new medium. The transfected cells were monitored daily for the development of CPE. The reconstituted virus was designated as CHV/BAC2.

2.6. Restriction enzyme analysis and Southern blotting

Genomic viral DNAs were treated overnight with restriction endonucleases at 37 °C. The digested DNAs were subjected to electrophoresis at 25 mA for 14 h at 4 °C on a 0.5% agarose gel. After electrophoresis, the gels were stained with ethidium bromide (1 μg/ml) and photographed on a UV-light transilluminator. The DNA fragments were transferred to Hybond-N^+ membranes (Amersham Biosciences) by capillary action. The blots were hybridized with the appropriate DNA probes labeled using the AlkPhos DIRECT labeling kit (Amersham Biosciences) according to the manufacturer's instructions, and detected using the CDP-Star detection reagent (Amersham Biosciences).

2.7. Modification of pCHV/BAC in E. coli

Recombination in *E. coli* was performed using the λ phage RED recombination system [37]. First, the gC open reading frame (ORF) was amplified from the purified CHV genome DNA using the primers: gCf, 5′-atgagttttaaaaatttttatct-3′ and gCr, 5′-ttagatcttattatttttttgaaC-3′. The amplified fragment was cloned into the pCR2.1TOPO (Invitrogen) using the TA cloning system and was designated as pCRgC. The minimal kanamycin resistance cassette (Kan^r) was amplified by PCR from the linear vector, pCR2.1 (Invitrogen) using the following primers: 5′-cccggGAAGTTCCTATTCTCTAGAAAGTATAGGAACTTCgacagcaagcgaaccggaat-3′ and 5′-cccggGAAGTTCCTATACTTTCTAGAGAATAGGAACTTCcggaaatgttgaatactcatactcttcctttttc-3′, and each primer was phosphorylated before being subjected to PCR. Each primer contains the Flp recognition target (FRT) site (upper case) and an *Sma*I site for subsequent ligation. The PCR product was purified and ligated into pCRgC, which had been digested with *Hin*cII and *Cla*I, blunt-ended by Klenow, and dephosphorylated. The resultant plasmid was amplified by the primer set of gCf and gCr, purified and resuspended in sterile water. This fragment has the arms of the gC ORF and contains Kan^r flanked by two FRT sites in the middle of the ORF. The pCHV/BAC DNAs from DH10B were electroporated into *E. coli* strain EL250 (kindly provided from Dr. N. G. Copeland, National Cancer Institute-Frederick, Frederick, MD, USA). The growth property of the reconstituted virus was checked to be equal to that from DH10B. The preparation of electrocompetent EL250 cells, in which pCHV/BAC was maintained, was performed as described below [38]. Overnight cultures of bacteria that contained pCHV/BAC were grown from a single colony, diluted 50-fold in LB medium, and grown until the OD_{600} of the culture was 0.5 at 32 °C. The cultures were then induced to express the Beta, Exo, and Gam proteins at 42 °C for 15 min, followed by chilling on ice for 15 min. The cells were then centrifuged for 5 min and washed three times with ice-cold sterile water. After washing, the cells were resuspended in ice-cold sterile water, added to 300 ng of the PCR product, and electroporated under the conditions described above. Recombinant colonies were identified by plating on LB plates that contained 12.5 μg/ml Cm and 50 μg/ml kanamycin

(Kan). Recombination was verified by PCR and the electrophoresis pattern of the genome, and the recombinant DNA was designated as pCHV/BAC–ΔgCkm. The pCHV/BAC–ΔgCkm construct was transfected into A-72 cells and the progeny virus was designated as CHV/BAC–ΔgCkm.

2.8. Removal of the kanamycin resistance cassette

Colonies that carried the correct BAC were inoculated into LB medium that contained Cm and Kan and cultured overnight. The cultures were then diluted 50-fold in LB medium and incubated until the OD_{600} was 0.5. The culture was induced by the addition of 0.1% L-arabinose (Sigma Aldrich, St. Louis, MO), incubated for 1 h, diluted, and plated on LB plates that contained Cm. After overnight incubation, colonies were picked and transferred to plates that contained either Cm or Kan. Recombinant clones, which were selected for growth on the plate with Cm, were confirmed by PCR and the electrophoresis pattern after *Eco*RI digestion. Purified DNA samples from the positive clones (pCHV/BAC–ΔgC) were transfected into A-72 cells. The progeny virus was designated as CHV/BAC–ΔgC.

2.9. BAC excision

To test whether the BAC DNA backbone flanked by two loxP sites was excisable from the viral genome, MDCK cells were infected with the recombinant adenovirus AxCANCre, which expresses Cre recombinase, at an M.O.I. of 50. After 2 h, the cells were washed and maintenance medium was added. At 24 h post-infection, the cells were superinfected with CHV/BAC or CHV/BAC–ΔgC at an M.O.I. of 0.03. After an additional 24 h, the supernatants were harvested, diluted, and incubated with MDCK cells for 3 days. The progeny virus was plaque-purified based on lack of expression of GFP, and designated as CHV/dBAC or CHV/dBAC–ΔgC, respectively.

2.10. Replication kinetics

Confluent monolayers of MDCK cells were infected with the DFD-6 wild-type (wt) or recombinants at an M.O.I. of 0.01 or 1.0 for 1 h at 37 °C. Uninfected virus was removed by aspiration, and the infected cells were washed with PBS and overlaid with maintenance medium. At different time-points post-infection (p.i.), the cells and supernatants were harvested, and the cells were frozen and thawed once, followed by centrifugation to collect intracellular viruses. Fifty percent tissue culture infectious dose ($TCID_{50}$) values were determined in A-72 cells. The experiments were performed in triplicate.

2.11. Plaque morphology and plaque size

To examine differences in plaque morphology between DFD-6 (wt) and the recombinants, CHV/BAC, CHV/dBAC or CHV/BAC–ΔgC, 5×10^5 cells were seeded onto six-well plates and cultured in growth medium for 3 days. Then, the MDCK cells were infected with viruses and cultured with medium that contained 0.5% methylcellulose and 0.01% DEAE-dextran. Three days later, the plaques were observed for GFP expression under a fluorescence microscope. The average size of plaques in MDCK cells was measured after 5 days post-infection. Fifty plaques were randomly selected and the size of them was measured by using NIH Image software. Student's *t*-test was employed to compare the mean plaque sizes of the viruses examined.

3. Results

3.1. Generation of recombinant viruses and BAC plasmids

We have cloned the CHV genome into a BAC. To this end, the recombinant plasmid pCTKdEHBAC, which contains the BAC vector sequences and the selection marker GFP-expressing cassette between the loxP sites and is flanked by the viral sequence comprising the U_L21, 22, 23 (TK), and 24 genes, was constructed. The flanking sequence provided the substrate for homologous recombination between the BAC and the CHV genome. The BAC vector sequences comprise a chloramphenicol resistance gene (Cm^r) and elements from the *E. coli* F factor, which are required for the stable maintenance and partition of large plasmids in *E. coli* [39]. The linearized recombination plasmid pCTKdEHBAC was transfected into MDCK cells, followed by infection with CHV. The correct insertion of the BAC vector should result in the formation of a recombinant CHV/BAC (Fig. 1A). CHV/BAC was selected under fluorescence microscopy based on the expression of GFP (Fig. 6A). As shown in Fig. 2A, the 6.3-kb of the BAC sequence was confirmed by *Sal*I digestion. To confirm that the foreign genes were inserted in the correct position in the TK gene, the CHV/BAC genome was digested with *Eco*RI, and as expected, the 9.8-kb fragment [8] of the CHV genome, into which the foreign genes had been inserted, was fused into a fragment of approximately 15.6 kb (Fig. 2A). These results indicate that the foreign gene is inserted correctly in the TK gene and that the construction of CHV/BAC is as expected.

Circular intermediates of the recombinant viral genome were isolated from infected cells using the Hirt extraction procedure, and the DNA was electroporated into *E. coli* DH10B (Fig. 1B). A BAC that carried the CHV genome, pCHV/BAC, was isolated from the chloramphenicol-resistant bacterial clones. To reconstitute infectious virus, the BAC plasmid pCHV/BAC was transfected into A-72 cells (Fig. 1B). Viral plaques typically appeared 4–5 days after transfection. The *Xba*I restriction patterns of the genomes of reconstituted CHV/BAC2 and parental CHV/BAC showed no differences (Fig. 2B). These results confirm the cloning of the CHV genome as an infectious BAC in *E. coli*.

To test whether the BAC DNA backbone flanked by two loxP sites was excisable from the viral genome, MDCK cells were infected with the recombinant adenovirus AxCANCre,

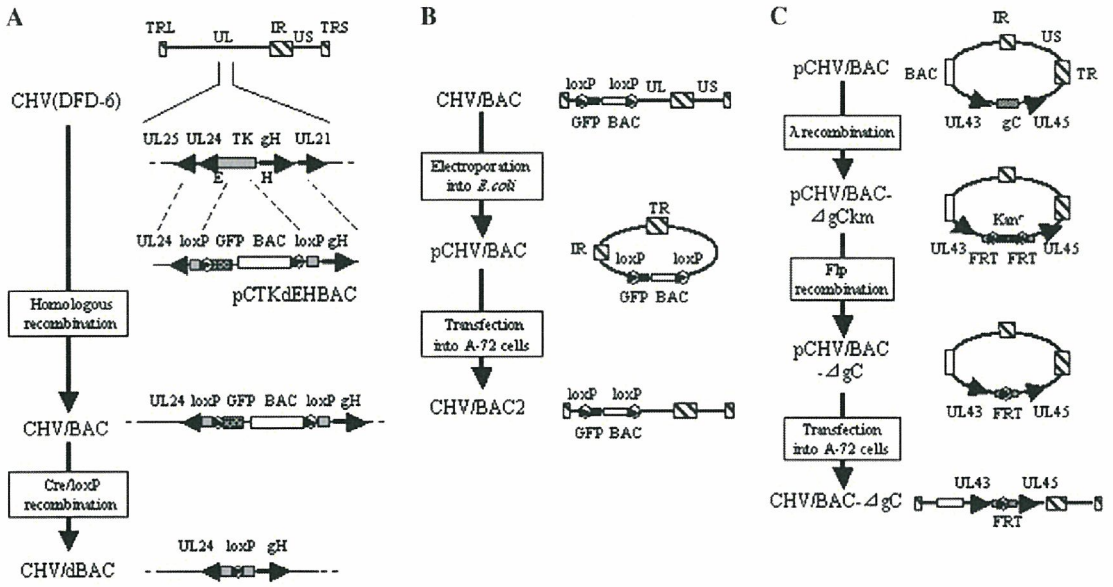

Fig. 1. Strategy to clone the CHV genome into a BAC. Schematic representation of the genomic arrangement of CHV DFD-6 and the relevant domains of the recombinant viruses and CHV/BACs. (A) A linear diagram of the CHV genome and expanded sections of the domain that encodes UL21 to UL25. The GFP expression cassette (GFP) and BAC sequence (BAC) were inserted into the TK locus by homologous recombination with the transfer vector that carries the GFP/BAC sequence flanked by loxP sites and excised by Cre/loxP recombination with a recombinant adenovirus that expresses the Cre recombinase. These recombination steps were carried out in MDCK cells. The unique sequences are represented as unique long (UL) and short (US) sequences, and the flanking repeats are shown as rectangles, which designate terminal repeat long (TRL) and short (TRS) and internal repeats (IR). (B) Schematic representation of the reconstitution of the CHV infectious clone. The genomic DNA of CHV/BAC was electroporated into *E. coli* DH10B and the pCHV/BAC DNA was transfected into A-72 cells to reconstitute the virus (CHV/BAC2). (C) Schematic representation of the deletion of gC from CHV/BAC. The PCR fragment that contains the kanamycin resistance cassette (Kan^r) and FRT sites flanked by homologous sequences of gC was inserted into the gC locus of pCHV/BAC using the λ phage RED recombination system (CHV/BAC−ΔgCkm). These recombination steps were carried out in *E. coli* EL250 by means of positive selection with kanamycin. Furthermore, Kan^r was removed by Flp recombination in the absence of kanamycin, thereby generating pCHV/BAC−ΔgC. pCHV/BAC−ΔgC was transfected into A-72 cells to produce the infectious virus (CHV/BAC−ΔgC). The positions of the gC gene located between UL43 and UL45, as well as the Kan^r and FRT sites are shown.

which expresses Cre recombinase, and then superinfected with CHV/BAC. Some of the progeny viruses did not express GFP. One plaque that did not express GFP was purified and designated as CHV/dBAC (Fig. 6A).

The insertion of the BAC sequence into the CHV genome and its subsequent removal were confirmed by Southern blotting analysis (Fig. 3B). The PCR products amplified from the Cm^r gene were labeled using the AlkPhos DIRECT labeling kit and hybridized to the genomic DNAs of DFD-6, CHV/BAC or CHV/dBAC, all of which had been digested with *Eco*RI (Fig. 3B, lanes 1, 2, and 3). As expected, the probe hybridized only to the 15.6-kb and 2.1-kb DNA fragments from CHV/BAC. As described above, the BAC sequence was inserted into the 9.8-kb *Eco*RI fragment. The Cm^r sequence in the BAC sequence originally contained an *Eco*RI site, and the probe hybridized to the DNA fragments that included the partial sequence of the BAC (15.6 kb) and the GFP-expressing cassette (2.1 kb) (Fig. 3A). The insertion of the BAC sequence was confirmed using another probe. The probe derived from the TK gene hybridized to the genomic DNA that had been digested with *Hin*dIII (Fig. 3B, lanes 4, 5, and 6). In the wild-type, the TK gene is located on fragments f (6.3 kb) and j (4.4 kb), which result from digestion of the CHV genome with *Hin*dIII [8]. The *Hin*dIII site in the TK gene disappeared following conjugation of the TK gene, the GFP gene, and the

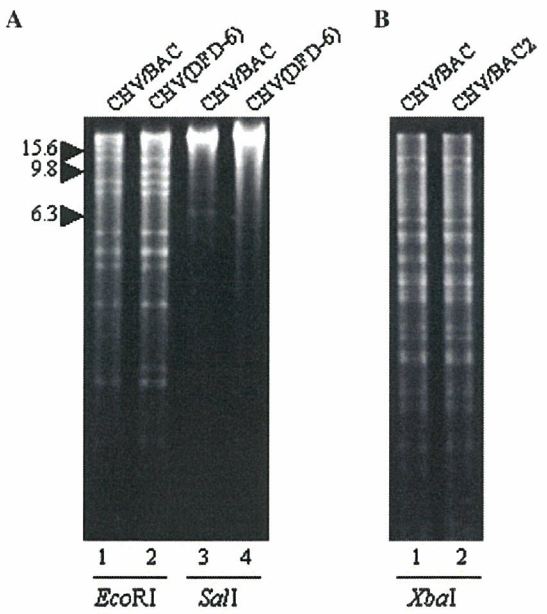

Fig. 2. Restriction analysis. The digested fragments were separated in 0.5% agarose gels. The fragment sizes are indicated in kilobase pair at the left-hand side. (A) Purified viral DNA of CHV/BAC or DFD-6 was digested with *Eco*RI or *Sal*I. (B) Comparison of the restriction digestion patterns of CHV/BAC and CHV/BAC2. The viral DNAs were digested with *Xba*I.

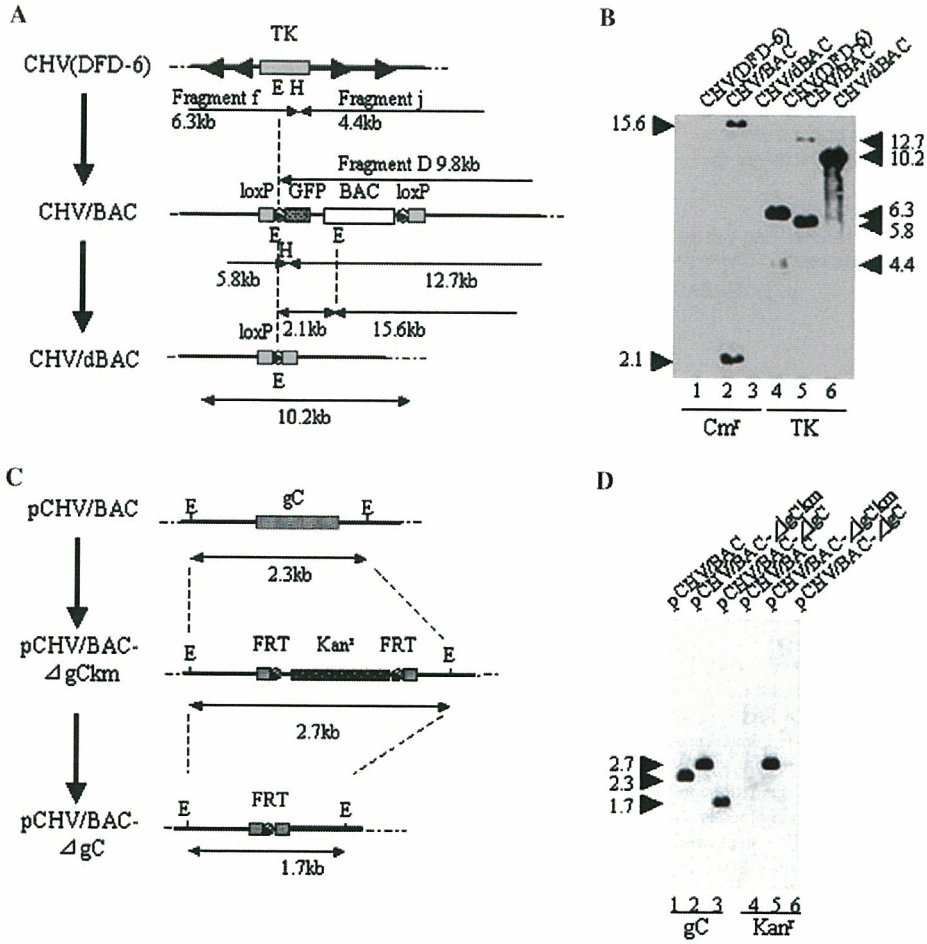

Fig. 3. Southern blot analysis of the recombinant genomes. The fragments were separated in 0.5% agarose gels. The fragment sizes are indicated in kilobase pair at the right-hand or left-hand sides. (A) Schematic representation of the domains of the recombinant viruses relevant to the construction of CHV/BAC and CHV/dBAC. The *Eco*RI (E) and/or *Hin*dIII (H) fragments are indicated. (B) Purified DNAs from the viruses were digested with *Eco*RI (lanes 1, 2, and 3) or *Hin*dIII (lanes 4, 5, and 6). The fragments were transferred onto nylon membranes for Southern blotting with probes specific for Cm^r (lanes 1, 2, and 3) or the TK gene (lanes 4, 5, and 6). (C) Schematic representation of the relevant domains of the BAC DNAs used in generating CHV/BAC−ΔgCkm and CHV/BAC−ΔgC. The *Eco*RI (E) fragment is indicated. (D) The DNAs from EL250 were digested with *Eco*RI and hybridized with probes specific for gC (lanes 1, 2 and 3) or Kan^r (lanes 4, 5, and 6).

BAC sequence. However, the *Hin*dIII site re-appeared between the loxP site and the GFP gene. Thus, the size of subfragment f in the CHV/BAC genome decreased to 5.8 kb. Since the *Hin*dIII site inside the two loxP sites disappeared following the removal of the BAC sequence, fragments f and j fused and a 10.2-kb subfragment appeared in the CHV/dBAC genome (Fig. 3A). The subfragment derived from fragment j was detected as a faint 4.4-kb or 12.7-kb band, as the result of digestion of DFD-6 or the CHV/BAC genome with *Hin*dIII, respectively (Fig. 3B, lanes 4 and 5).

3.2. Site-specific recombination of the CHV infectious clone

Recently, the λ recombination system has been used to modify efficiently and specifically genes carried by BACs in *E. coli* [37]. To determine whether this procedure is adaptable to the modification of pCHV/BAC, the gene that encodes glycoprotein C of CHV was targeted for deletion. The pCHV/BAC construct purified from DH10B was electroporated into EL250, which expresses Beta, Exo, and Gam at 42 °C, and flp recombinase was induced by the addition of L-arabinose. The targeting cassette, which contained the Kan^r gene flanked by two FRT sites and a sequence homologous to the gC gene, was constructed by PCR. The purified PCR product was electroporated into EL250 cells that contained pCHV/BAC. After electroporation, the cells were plated on medium that contained Cm and Kan for the positive selection of pCHV/BAC−ΔgCkm. Furthermore, to remove the Kan^r sequence from CHV/BAC−ΔgCkm, the EL250 clone that contained pCHV/BAC−ΔgCkm was induced with L-arabinose and clones that grew on the Cm-containing plate but not on the Kan-containing plate were selected. The recombinant virus CHV/BAC−ΔgC was obtained from one of these clones (Fig. 1C).

The genomes of CHV/BAC and the two modified BACs, CHV/BAC−ΔgCkm and CHV/BAC−ΔgC, were purified by

the methods developed by Sinzger et al. [34], and the recombinants were confirmed by sequence analysis and the electrophoresis patterns following DNA digestion with *Eco*RI (data not shown). The BAC DNAs from EL250 were analyzed by Southern blotting (Fig. 3D). The probes were constructed from PCR products that contained the gC gene (Fig. 3D, lanes 1, 2, and 3) or Kan^r gene (Fig. 3D, lanes 4, 5, and 6). As expected, the probe that contained the gC sequence hybridized with the 2.3-kb fragment derived from pCHV/BAC, whereas it hybridized with the 2.7-kb fragment derived from pCHV/BAC−ΔgCkm and the 1.7-kb fragment derived from pCHV/BAC−ΔgC, respectively (Fig. 3C). The Kan^r-specific probe hybridized only with the 2.7-kb fragment that was derived from pCHV/BAC−ΔgCkm, indicating that insertion and excision of the Kan^r cassette occurred as expected.

3.3. Characterization of recombinant viruses

To determine the effects of insertion, the replication kinetics of the recombinants were compared to that of the parental strain DFD-6. Monolayers of MDCK cells were infected at an M.O.I. of 1 or M.O.I. of 0.01. The titer of CHV/BAC decreased at every time-point compared to that of the wild-type DFD-6 (Fig. 4A and B). However, when infected at an M.O.I of 1, the differences between the virus titers were smaller than the standard errors (Fig. 4A), while the difference in titer was more than 10-fold when the cells were infected at an M.O.I of 0.01 (Fig. 4B). This reduction of the titer seems to be caused by deletion of the TK gene because growth properties of CHV/BAC and CHV/dBAC are identical even when infected at an M.O.I. of 0.01 (Fig. 5A and B).

The CHV/BAC−ΔgC or CHV/dBAC−ΔgC titers were markedly reduced at every time-point compared to CHV/BAC or CHV/dBAC, which contains gC, with respect to the viral titers in both the supernatants and the infected cells. We investigated only a low M.O.I. for CHV/BAC−ΔgC or CHV/dBAC−ΔgC because the titer of this recombinant virus could not be increased sufficiently to prepare stock virus for infection at an M.O.I. of 1. These data demonstrate that the gC of CHV is not essential for CHV replication, while the deletion of gC impairs severely the growth of the virus.

To characterize the recombinants, MDCK cells were infected with the viruses and observed 3 days later. The plaques for CHV/BAC and CHV/dBAC appeared to be slightly smaller than those for DFD-6 ($p < 0.01$), although the shapes of the plaques were not different (Fig. 6A and B). Plaque morphology and size of CHV/BAC was identical to that of CHV/dBAC (data not shown). However, in the case of CHV/BAC−ΔgC, the plaque morphology was not circular and the plaque size was smaller than that of CHV/BAC ($p < 0.01$, Fig. 6A and B).

4. Discussion

We have succeeded in cloning the CHV genome as a BAC (pCHV/BAC). This is the first report describing the construction of a BAC for use as a basal vector in a recombinant vaccine or prospective gene therapy for companion animals. The salient findings are summarized below.

The excision of the BAC sequence from the CHV genome is necessary, as reported by several groups studying the BACs of other herpesviruses [14,27,40]. In the present study, since the GFP and BAC sequences were designed to be surrounded by two loxP sites, we could easily select CHV/BAC in the majority of the wild-type DFD-6 clones by picking a GFP-positive plaque. Subsequently, the BAC sequence and GFP were easily deleted by the Cre/loxP recombination system. Therefore, this selection system with GFP can be used to ascertain whether or not the BAC sequence is deleted from the CHV genome and is applicable to carrying out recombination in herpesviruses, towards the goal of producing BACs.

The pCHV/BAC construct could be manipulated in *E. coli*. Insertion of the exogenous gene (Kan^r gene with flanking FRT sites) and deletion of an endogenous gene (for glycoprotein C) in pCHV/BAC were conducted in *E. coli* strain EL250 using λ recombination followed by Flp recombination. Although

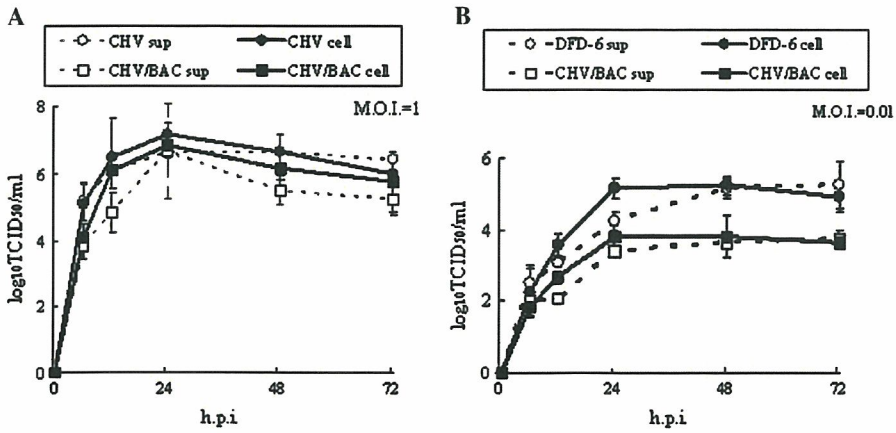

Fig. 4. Growth kinetics of CHV/BAC. Monolayers of MDCK cells were infected with DFD-6 or CHV/BAC. The cells or supernatants were recovered at 6, 12, 24, 48, and 72 h p.i. and $TCID_{50}$ was determined using A-72 cells. The experiments were performed in triplicate. Shown are data on $TCID_{50}$ of recombinant viruses from cells and supernatants with standard errors. (A) Cells were infected at an M.O.I. of 1. (B) Cells were infected at an M.O.I. of 0.01.